



HAL
open science

Persistence of Integrase-Deficient Lentiviral Vectors Correlates with the Induction of STING-Independent CD8+ T Cell Responses

Céline Cousin, Marine Oberkamp, Tristan Felix, Pierre Rosenbaum, Robert Weil, Sylvie Fabrega, Valeria Morante, Donatella Negri, Andrea Cara, Gilles Dadaglio, et al.

► **To cite this version:**

Céline Cousin, Marine Oberkamp, Tristan Felix, Pierre Rosenbaum, Robert Weil, et al.. Persistence of Integrase-Deficient Lentiviral Vectors Correlates with the Induction of STING-Independent CD8+ T Cell Responses. *Cell Reports*, 2019, 26 (5), pp.1242-1257.e7. 10.1016/j.celrep.2019.01.025 . pasteur-02001260

HAL Id: pasteur-02001260

<https://pasteur.hal.science/pasteur-02001260>

Submitted on 31 Jan 2019

HAL is a multi-disciplinary open access archive for the deposit and dissemination of scientific research documents, whether they are published or not. The documents may come from teaching and research institutions in France or abroad, or from public or private research centers.

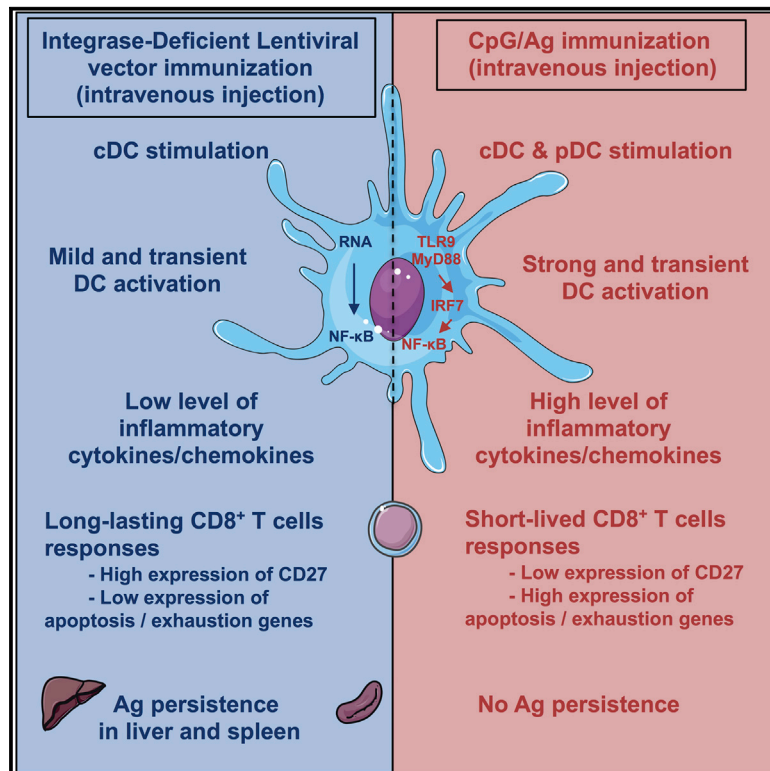
L'archive ouverte pluridisciplinaire **HAL**, est destinée au dépôt et à la diffusion de documents scientifiques de niveau recherche, publiés ou non, émanant des établissements d'enseignement et de recherche français ou étrangers, des laboratoires publics ou privés.



Distributed under a Creative Commons Attribution 4.0 International License

Persistence of Integrase-Deficient Lentiviral Vectors Correlates with the Induction of STING-Independent CD8⁺ T Cell Responses

Graphical Abstract



Authors

Céline Cousin, Marine Oberkamp, Tristan Felix, ..., Andrea Cara, Gilles Dadaglio, Claude Leclerc

Correspondence

gilles.dadaglio@pasteur.fr (G.D.),
claud.leclerc@pasteur.fr (C.L.)

In Brief

Lentiviruses (LVs) are among the most promising vaccine vectors. To develop safer LV-derived vaccines, integrase-deficient LVs (IDLVs) have been recently generated. Cousin et al. show here that IDLVs induce strong and persistent cytotoxic T cell responses and decipher the mechanisms by which IDLVs induce efficient adaptive immune responses.

Highlights

- Integrase-deficient lentiviral vectors overcome the risk of insertional mutagenesis
- IDLVs induce strong and persistent specific cytotoxic T cell responses
- IDLVs persist several months in spleen and liver of vaccinated mice
- The CTL responses induced by IDLVs require NF-κB signaling in CD11c⁺ dendritic cells



Persistence of Integrase-Deficient Lentiviral Vectors Correlates with the Induction of STING-Independent CD8⁺ T Cell Responses

Céline Cousin,^{1,2} Marine Oberkampff,^{1,2} Tristan Felix,^{1,2,7} Pierre Rosenbaum,^{1,2} Robert Weil,³ Sylvie Fabrega,⁴ Valeria Morante,⁵ Donatella Negri,⁵ Andrea Cara,⁶ Gilles Dadaglio,^{1,2,8,*} and Claude Leclerc^{1,2,8,9,*}

¹Institut Pasteur, Unité de Régulation Immunitaire et Vaccinologie, Equipe Labellisée Ligue Contre le Cancer, 75015 Paris, France

²INSERM U1041, 75015 Paris, France

³Institut Pasteur, Unité Signalisation et Pathogénèse, Département Biologie Cellulaire et Infection, 75015 Paris, France

⁴Plateforme Vecteurs Viraux et Transfert de Gènes, SFR Necker, US 24, UMS 3633, 75014 Paris, France

⁵Department of Infection Diseases, Istituto Superiore di Sanità, Rome, Italy

⁶National Center for Global Health, Istituto Superiore di Sanità, Rome, Italy

⁷Present address: IHU Imagine, Institut des Maladies Génétiques, Equipe “Chromatin and gene regulation during development,” 75015 Paris, France

⁸These authors contributed equally

⁹Lead Contact

*Correspondence: gilles.dadaglio@pasteur.fr (G.D.), claud.leclerc@pasteur.fr (C.L.)

<https://doi.org/10.1016/j.celrep.2019.01.025>

SUMMARY

Lentiviruses are among the most promising viral vectors for *in vivo* gene delivery. To overcome the risk of insertional mutagenesis, integrase-deficient lentiviral vectors (IDLVs) have been developed. We show here that strong and persistent specific cytotoxic T cell (CTL) responses are induced by IDLVs, which persist several months after a single injection. These responses were associated with the induction of mild and transient maturation of dendritic cells (DCs) and with the production of low levels of inflammatory cytokines and chemokines. They were independent of the IFN- γ , TLR/MyD88, interferon regulatory factor (IRF), retinoic acid induced gene I (RIG-I), and stimulator of interferon genes (STING) pathways but require NF- κ B signaling in CD11c⁺ DCs. Despite the lack of integration of IDLVs, the transgene persists for 3 months in the spleen and liver of IDLV-injected mice. These results demonstrate that the capacity of IDLVs to trigger persistent adaptive responses is mediated by a weak and transient innate response, along with the persistence of the vector in tissues.

INTRODUCTION

An ideal vaccine has to deliver the antigen to professional antigen-presenting cells (APCs) in the context of appropriate costimulation and cytokine stimulus in order to induce potent primary and memory immune responses. In particular, dendritic cells (DCs) must efficiently capture the antigen and receive maturation signals. Indeed, although immature DCs induce T cell tolerance, the presence of costimulating signals and inflammatory cyto-

kines results in the potent induction of immunity (Bonifaz et al., 2002; Probst et al., 2003).

Several viral vectors, such as adenoviruses, adeno-associated viruses, and lentiviral vectors (LVs) (Nayak and Herzog, 2010), have been used to deliver antigens to DCs, generating efficient immune responses against pathogens and tumors. LVs are a subclass of retroviral vectors derived from HIV-1. They have been developed in order to generate self-inactivating vectors, without pathogenic or replicative capacity, while maintaining their ability to transfer and integrate into the host genome (Zufferey et al., 1998).

Compared to other gene delivery technologies, LVs possess major advantages. Indeed, their immunogenicity can be decreased by the deletion of selected genes, and there is usually no pre-existing immunity against LVs (Sakuma et al., 2012; Vigna and Naldini, 2000). *In vitro*, both murine and human DCs can be transduced with LVs with efficiencies of 30% to 90% (Esslinger et al., 2002; Chinnasamy et al., 2000) for the activation of CD8⁺ T cells (Esslinger et al., 2002; He et al., 2005). LVs thus represent a very attractive platform for *in vivo* gene delivery, either for vaccination (Beignon et al., 2009) or to correct genetic defects (Aiuti et al., 2013; Biffi et al., 2013). Gamma-retroviral vectors have been successfully used to treat children with X-linked severe combined immunodeficiency (Hacein-Bey-Abina et al., 2003). However, acute leukemia developed in four of these patients, demonstrating that the main drawback of these vectors is the risk of insertional mutagenesis (Hacein-Bey-Abina et al., 2010). Conversely, to date, there has only been a single case of insertion-dependent clonal expansion in lentiviral transduction in gene therapy cases despite hundreds of gene therapy patients (Cartier et al., 2009).

To develop safer LV-derived vectors, integrase-deficient LVs (IDLVs) have been recently generated through the use of mutations in the integrase protein that minimize proviral integration (Sakuma et al., 2012; Philippe et al., 2006; Vargas et al., 2004). Several reports have demonstrated that nonintegrative IDLVs induce



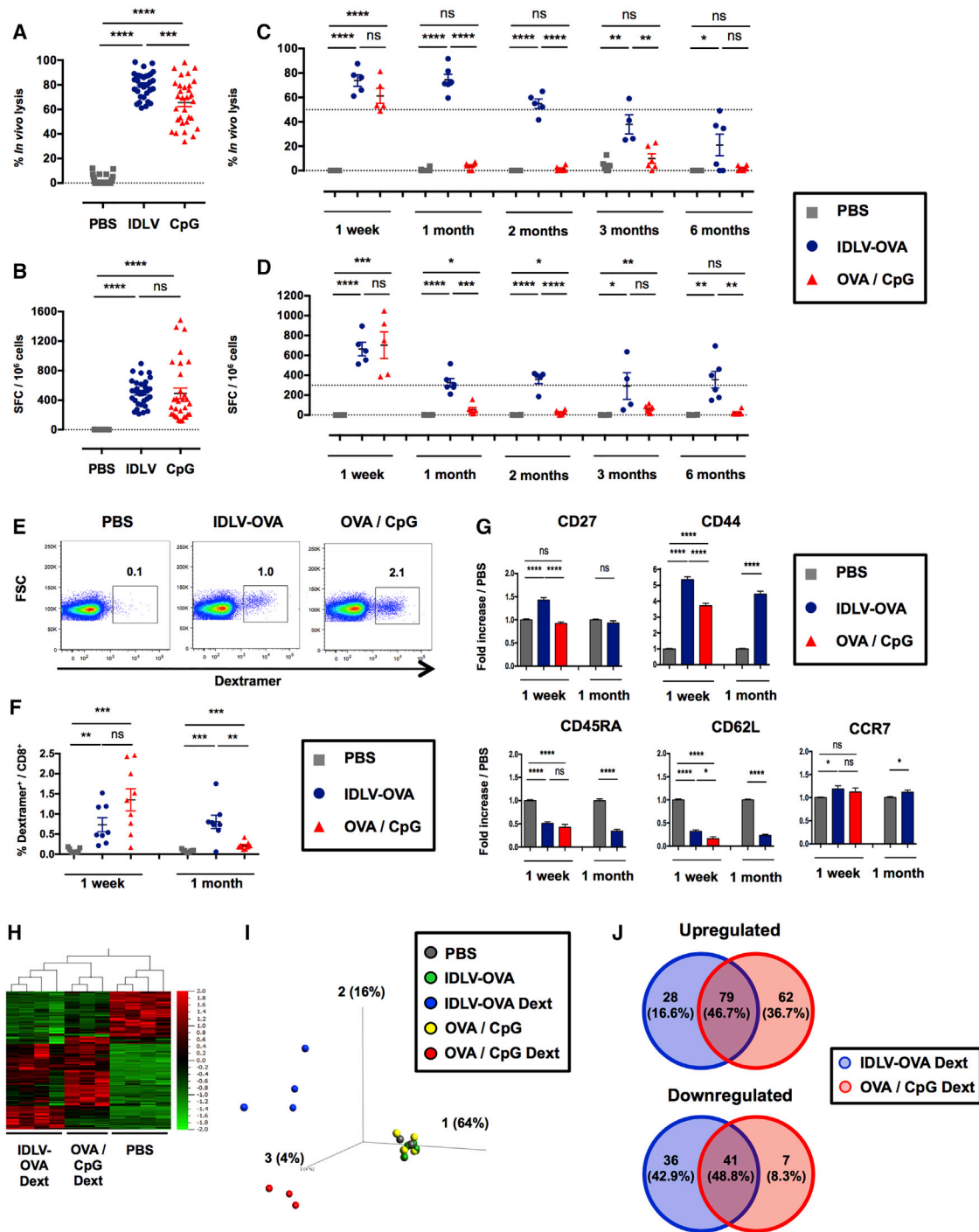


Figure 1. IDLV-OVA Induces Sustained and Persistent CTL Responses

C57BL/6 mice were injected intravenously (i.v.) with PBS, 10^6 TUs IDLV-OVA or OVA plus CpG.

(A and B) Seven days later, anti-OVA CTL responses were assessed by an *in vivo* killing assay (A) and IFN- γ ELISPOT (B).

(C and D) The persistence of the anti-OVA CTL responses was assessed by an *in vivo* killing assay (C) and IFN- γ ELISPOT (D) up to 6 months after immunization.

(A–D) The results are expressed as the percentage of specific lysis for the *in vivo* killing assay (A and C) and IFN- γ spot-forming cells (SFC) per 10^6 splenocytes for ELISPOT (B and D). Each dot represents an individual mouse. The results represent the means \pm SEM of cumulative data from 33 mice from eleven independent experiments (A and B) or from 6 mice from two independent experiments (C and D).

(E–G) Seven days and 1 month later, the OVA-specific CD8 $^+$ T cell response was analyzed by H-2K b /SIINFEKL-Dextramer staining. The gating strategy for CD3 $^+$ CD8 $^+$ CD4 $^-$ dextramer positive cells 1 week after immunization is shown in (E).

(legend continued on next page)

strong immune responses that can be used in protective immunization against infectious diseases and for tumor immunotherapy (Negri et al., 2007; Karwacz et al., 2009; Grasso et al., 2013).

The mechanisms by which LVs induce these strong adaptive immune responses remain controversial. Indeed, the maturation of DCs is regulated by various signals that are sensed by pattern recognition receptors (PRRs), including Toll-like receptors (TLRs), retinoic acid-induced gene (RIG)-I-like receptors (RLRs), DNA sensors, nucleotide-binding oligomerization domain-like receptors (NLRs), and C-type lectin receptors (CLRs) (Gürtler and Bowie, 2013; Fritz et al., 2006; Geijtenbeek and Gringhuis, 2009). HIV-1 has a single-stranded positive RNA (ssRNA) genome (Sakuma et al., 2012) that can be directly detected in the cytosol by the retinoic acid induced gene I (RIG-I) receptor or by TLR7 in the endocytic compartment (Pichlmair et al., 2006; Diebold et al., 2004). In addition, ssRNA can also be converted by RNA polymerase III into double-stranded RNA (dsRNA), which is a natural ligand of TLR3 (Alexopoulou et al., 2001). This mechanism is involved in the innate sensing of LVs by DCs (Breckpot et al., 2010). Furthermore, *in vitro* studies have suggested that the type I interferon (IFN-I) response to HIV-1 is due to the activation of TLR7 on plasmacytoid DCs (pDCs) by the viral ssRNA genome (Beignon et al., 2005). Thus, LVs can directly activate pDCs through the engagement of TLR7 and TLR9, leading to IFN- α production, which, in turn, promotes the bystander maturation of myeloid DCs (Rossetti et al., 2011). Furthermore, by-products present in the vector preparation, such as tubulovesicular structures containing nucleic acids, can stimulate TLR9, leading to the production of IFN-I by pDCs (Pichlmair et al., 2007). Double-stranded DNA (dsDNA) generated after reverse transcription of the viral genome by the viral reverse transcriptase (Sakuma et al., 2012) could be detected by cytosolic DNA sensors that act upstream of stimulator of interferon genes (STING) (Gürtler and Bowie, 2013). As a result, LV proviral DNA could trigger both TLR- and non-TLR-mediated pathways (Agudo et al., 2012). Very recently, Kim et al. demonstrated that the induction of efficient immune responses by LVs is mediated by DC activation following the pseudotransduction of LV particles in a phosphoinositide 3-kinase (PI3K)-dependent process and by the cellular DNA package from LV preparation through a STING and cyclic guanosine monophosphate-AMP (cGAS) pathway (Kim et al., 2017).

In the present study, using IDLVs expressing ovalbumin (IDLV-OVA) as a model antigen, we confirmed that IDLVs can induce strong cytotoxic T cell (CTL) responses, which persist several months after a single injection in the absence of an adjuvant. These strong responses were associated with the *in vivo* induction of mild and transient maturation of both conventional DCs (cDCs) and pDCs and with the production of low levels of inflammatory cytokines and chemokines. Only cDCs were required for the induction of CTL responses by IDLVs. This induction was independent of the main signaling pathways that can be potentially activated by IDLVs, i.e., TLR and MyD88, interferon regulatory factor (IRF), RIG-I, and STING, but were fully dependent upon nuclear factor κ B (NF- κ B) signaling in CD11c⁺ cells. In addition, we demonstrated that, despite their lack of integration, IDLV-OVA persisted in the spleen and the liver of vaccinated mice up to 3 months after vaccination via intravenous injection. This study thus demonstrates that potent adaptive immune responses can be triggered by IDLVs in the absence of marked and prolonged inflammatory responses, suggesting that the long-lasting CTL responses induced by IDLVs may be associated with the persistence of the transgene.

RESULTS

IDLV-OVA Induces Strong and Persistent CTL Responses

To analyze the CTL responses induced by IDLV-OVA, various doses of this recombinant IDLV were intravenously injected into C57BL/6 mice for comparison with OVA with cytosine-phosphate-guanine class B (CpG-B), a potent adjuvant used to induce CTL responses. The *in vivo* lysis as well as the number of IFN- γ -producing cells were analyzed 1 week later (Figures S1A and S1B). Strong CTL responses were detectable, even after the injection of a low dose of the vaccine. The optimal dose of 10⁶ transduction units (TUs) of IDLV-OVA was selected because this dose induced a high CTL response in all mice. In contrast, at 0.5 \times 10⁶ TUs and below, some mice were not responding in the IFN- γ enzyme-linked immunospot (ELISPOT) assay. Following immunization with the optimal dose of 10⁶ TUs, CTL responses were still detectable up to 6 months after vaccination (Figures 1A–1D). In contrast, the OVA-specific CTL response induced by OVA plus CpG peaked at 1 week and then declined very

(F) The percentage of CD3⁺ CD8⁺ dextramer⁺ cells among the total CD8⁺ cells is shown at 1 week and 1 month after immunization. The results represent the means \pm SEM of cumulative data from 8 to 9 mice from 3 independent experiments.

(G) Expression of CD27, CD44, CD45RA, CD62L, and CCR7 by CD3⁺ CD8⁺ dextramer⁺ cells. The results are expressed as the fold-increase in the mean fluorescence intensity (MFI) \pm SEM compared to PBS-injected mice and represent the cumulative data from 8 to 9 mice from three independent experiments. Statistical analysis was performed by unpaired Student's t test (ns $p > 0.05$, * $p < 0.05$, ** $p < 0.01$, *** $p < 0.001$, **** $p < 0.0001$).

(H–J) Seven days later, splenic CD8⁺ T cells were purified from PBS-, IDLV-OVA-, and OVA plus CpG-treated mice, whereas OVA-specific CD8⁺ T cells (H-2K^b/SIINFEKL-Dextramer⁺ CD8⁺) were purified from IDLV-OVA and OVA plus CpG immunized mice. RNA was extracted, and the expression of genes involved in the immune response was assessed with the nCounter Mouse Pan Cancer Immune Profiling Panel.

(H) Heatmap of genes significantly and differentially expressed by OVA-specific CD8⁺ T cells purified from IDLV-OVA or OVA plus CpG immunized mice (IDLV-OVA Dext and OVA plus CpG Dext, respectively) compared to CD8⁺ T cells purified from PBS-injected mice (PBS).

(I) PCA (principal component analysis) of genes significantly and differentially expressed by OVA-specific CD8⁺ T cells purified from IDLV-OVA or OVA plus CpG immunized mice (IDLV-OVA Dext and OVA plus CpG Dext, respectively) compared to CD8⁺ T cells purified from mice injected with PBS (PBS) or IDLV-OVA (IDLV-OVA) or OVA plus CpG (OVA plus CpG).

(J) Venn diagrams of upregulated (upper panel) and downregulated (lower panel) genes differentially expressed by IDLV-OVA Dext or OVA plus CpG Dext. The results represent the cumulative data from 4 to 5 mice from five independent experiments.

See also Figures S1 and S2.

rapidly. The ability of IDLV-OVA to prevent the growth of B16-OVA cells was then evaluated. C57BL/6 mice were immunized with IDLV-OVA and 6 months later were grafted with B16-OVA tumor cells. As compared to control mice, the survival of IDLV-OVA immunized mice was significantly improved, and 2 out of 6 mice remained tumor free until the end of the experiment (Figures S1C and S1D). These data demonstrate that the persistent CTL responses induced by IDLV-OVA provided a long-lasting protective anti-tumor immunity.

The phenotype of OVA-specific CD8⁺ T cells was analyzed by fluorescence-activated cell sorting (FACS) on H-2K^b/SIINFEKL-Dextramer⁺ cells at 1 week and 1 month after immunization (Figures 1E–1G). One week after immunization, IDLV-OVA primed a lower frequency of OVA-specific dextramer⁺ cells (0.73% of total CD8⁺ T cells) than OVA plus CpG (1.35% of the total CD8⁺ T cells) (Figures 1E and 1F). However, the OVA-specific dextramer⁺ cells were still detectable 1 month after vaccination with IDLV-OVA in contrast to mice immunized with OVA plus CpG (Figure 1F). One week after vaccination, OVA-specific CD8⁺ T cells induced by IDLV-OVA expressed a classical effector CTL phenotype (Wherry and Ahmed, 2004) (CD27^{high} CD44^{high} CD45RA^{low} CD62L^{low} CCR7^{low}), similar to the OVA-specific CD8⁺ T cells induced by OVA plus CpG (Figure 1G). However, the expression of CD27 and CD44 was significantly upregulated in CTL cells induced by IDLV-OVA compared to OVA plus CpG. One month after immunization, OVA-specific CD8⁺ T cells induced by IDLV-OVA expressed an effector-memory T cell phenotype (CD27^{low} CD44^{high} CD45RA^{low} CD62L^{low} CCR7^{low}) (Figure 1G). These results suggest that IDLV induced a more persistent CTL response than OVA plus CpG.

OVA-Specific CD8⁺ T Cells Induced by IDLV-OVA Display a Specific Transcriptomic Signature

We next compared the transcriptomic profile of OVA-specific CD8⁺ T cells purified from the spleens of mice injected 1 week before with IDLV-OVA or OVA plus CpG (Figure S2A). The expression of 800 genes was compared using the Nanostring technology. The hierarchical heatmap clustering analysis (Figure 1H) and principal-component analysis (PCA) (Figure 1I) showed that OVA-specific CD8⁺ T cells induced by IDLV-OVA or OVA plus CpG exhibited different gene expression profiles. To characterize more precisely the differences between the two treatments, we identified genes that were differentially up- or downregulated in OVA-specific CD8⁺ T cells purified from immunized mice compared to CD8⁺ T cells purified from PBS-injected mice. Only 79 genes (46.7% of total upregulated genes) and 41 genes (48.8% of total downregulated genes) of the upregulated or downregulated genes, respectively, were shared by OVA-specific CD8⁺ T cells after immunization with IDLV-OVA or OVA plus CpG, demonstrating that these CTL populations possess distinct gene expression profiles.

Among the 107 genes upregulated and the 77 genes downregulated in OVA-specific CD8⁺ T cells from mice immunized with IDLV-OVA (Figure 1J), 14 genes were significantly upregulated, whereas 9 genes were significantly downregulated compared to CpG/OVA (Figure S2B). While the significantly upregulated genes are involved in the activation of T lymphocytes (*Klrf1*) (Jamieson et al., 2002), the downregulated genes are involved

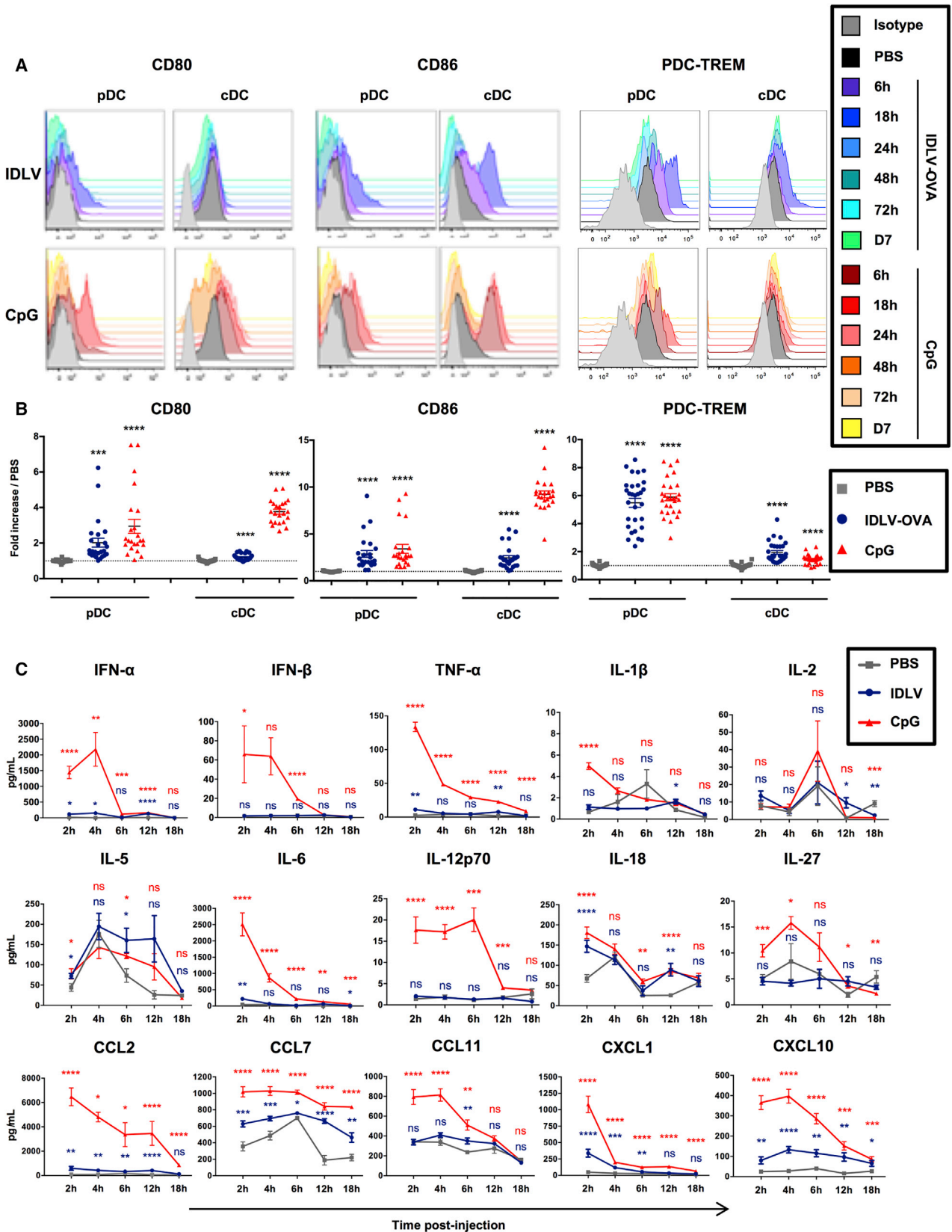
in T cell exhaustion (*Havcr2*, *Lag3*, and *Tigit*) (Wherry and Kurachi, 2015), apoptosis (*Casp3*) (Porter and Jänicke, 1999), and the activation of T lymphocytes (*Tnfrsf4*) (Watts, 2005). These results suggest that the activation of OVA-specific CTL by OVA plus CpG is followed by the exhaustion and apoptosis of CD8⁺ T cells, whereas the CTL induced by IDLV-OVA could be less activated and, thus, less prone to apoptosis, which could be correlated with the persistence of the CTL responses induced by IDLV-OVA. Thus, we then analyzed the expression of T cell exhaustion markers by OVA-specific CD8⁺ T cells. One week after immunization with IDLV-OVA or CpG/OVA, the expression of PD-1, CD153 (CD30-Ligand), CD223 (Lag3), and CD366 (Tim3) was analyzed by flow cytometry (Figure S2C). The expression of PD-1 and CD223 was significantly upregulated following immunization with IDLV-OVA or CpG/OVA, whereas the level of CD366 was strongly downregulated. However, no statistical difference was observed between specific CD8⁺ T cells induced either by IDLV-OVA or CpG/OVA immunization, suggesting that these markers were not involved in the exhaustion of CD8⁺ T cell responses induced by CpG/OVA.

IDLVs Induce a Mild and Transient Maturation of Mouse DCs

To understand the mechanisms responsible for the different gene expression profiles of the CD8⁺ T cells induced either by IDLV-OVA or OVA plus CpG, we next analyzed the innate responses induced by IDLV-OVA compared to CpG. Various doses of IDLVs were injected into mice, and we analyzed the expression by CD11c^{high}B220⁻ cDCs and CD11c^{low}B220⁺ CD317⁺Siglec-H⁺ pDCs (Figures S3A and S3B) of various activation markers and costimulatory molecules, as well as of molecules involved in the regulation of immune responses. After the injection of 5 × 10⁶ TUs IDLV-OVA, a significant but transient increase in the expression of CD80, CD86, and plasmacytoid DC-triggering receptor expressed on myeloid cells (PDC-TREM) by cDCs and pDCs was observed, which peaked 18 h after administration, whereas no significant effect was observed following the injection of lower doses (Figures S1B, 2A, and 2B). A significant increase in the expression of CD40, CD54, CD69, H-2K^b, I-A^b, ICOS-L, OX40-L, and PDL1 (Figures S3C–S3F) was also observed.

These results show that IDLV-OVA induces the maturation of both pDCs and cDCs. However, for some markers, this maturation was significantly less marked than in the CpG-treated mice. However, this was not true for CD80 (pDCs), CD86 (pDCs), I-A^b (pDCs), H-2K^b (cDCs), OX40-L, and PDC-TREM (pDCs). Furthermore, this was observed only after 5 × 10⁶ TUs but not after the administration of lower doses, which were capable of promoting the induction of strong CTL responses.

We then analyzed the cytokines and chemokines produced in the sera of vaccinated mice by using a Luminex assay (Figure S3G). The administration of CpG induced the production of high levels of most of the cytokines and chemokines tested (Figure 2C). The induction of IFN- γ , interleukin 2 (IL-2), and IL-12p70 were correlated with the expansion of highly cytolytic, terminally differentiated, short-lived effector CD8⁺ T cells (Cox et al., 2013). In contrast, IDLV-OVA treatment induced only the production of significant concentrations of IL-5 and IL-18, both of which were



(legend on next page)

required for an optimal CTL response (Cox et al., 2013; Apostolopoulos et al., 2000).

Altogether, these data show that strong and persistent CTL responses induced by IDLV-OVA are associated with a mild DC activation and a low and transient inflammation.

Conventional DCs Are Required for the Induction of CTL Responses by IDLV-OVA

Because both pDCs and cDCs were activated by IDLV-OVA, we analyzed their respective roles in the induction of CTL responses by using BDCA2-DTR (Swiecki et al., 2010) and CD11c-DTR (Jung et al., 2002) transgenic mice, which express the human diphtheria toxin receptor (DTR) under the control of BDCA2, a pDC-specific promoter, or the CD11c promoter, respectively. Because nonhematopoietic cells may also express the CD11c-DTR transgene (Jung et al., 2002), we produced chimeric mice (CD11c-DTR → wild-type [WT]) in which only the hematopoietic compartment is derived from CD11c-DTR mice. Administration of diphtheria toxin (DT) to BDCA2-DTR mice resulted in the depletion of pDCs, without affecting cDCs (Figures S4A and S4B). The treatment of CD11c-DTR → WT chimeric mice with DT induced the depletion of CD11c⁺ cells, i.e., cDCs and macrophages, but did not affect pDCs (Figures S4C–S4G). This finding was consistent with the results of a previous study (Hervas-Stubbs et al., 2014). The administration of DT to BDCA2-DTR mice had a low impact on the CTL responses (Figure 3A) or on the maturation of cDCs (Figures 3B, 3C, and S5) induced by IDLV-OVA but strongly reduced the adaptive and innate responses induced by OVA plus CpG. In contrast, the administration of DT to CD11c-DTR → WT chimeric mice fully abolished the CTL responses induced by IDLV-OVA (Figure 3D) and strongly reduced the maturation of pDCs (Figures 3E, 3F, and S5). The depletion of cDCs by DT treatment also suppressed the CTL responses induced by OVA plus CpG vaccination (Figure 3D) but did not affect the maturation of pDCs induced by the CpG (Figures 3E, 3F, and S5). Altogether, these results show that cDCs are strictly required for the induction of CTL responses by IDLV-OVA, whereas pDCs do not play a significant role.

The Induction of Immune Responses by IDLVs Is Independent upon IFN Signaling

IFN-I play a major role in the induction of CTL responses (Hervas-Stubbs et al., 2007). We, therefore, analyzed the CTL responses induced by IDLV-OVA in IFNAR-knockout (KO) mice, which are deficient in IFN-I receptors, compared to C57BL/6 mice (Figures 4A and 4B). The lack of IFN-I signaling did not affect the induction

of these responses either at 1 week (Figure 4A) or 1 month after immunization by IDLV-OVA (Figure 4B). In contrast, the CTL responses induced by OVA plus CpG were strongly decreased in IFNAR-KO mice, which is in agreement with our previous results (Hervas-Stubbs et al., 2007).

Whereas the CTL responses induced by IDLV-OVA were not affected in IFNAR-KO mice, the maturation of cDCs and pDCs was strongly decreased in these mice (Figures 4C–4F; Figure S6). A similar drastic reduction in DC maturation was observed in mice injected with CpG. These results demonstrate that the CTL responses induced by IDLVs are independent of IFN-I signaling and can be generated in the absence of the efficient maturation of cDCs.

The Induction of CTL Responses by IDLV-OVA Is Independent of the TLR3, TLR4, TLR7, TLR9, MyD88, IRF3, and IRF7 Pathways

IDLVs were produced in human embryonic kidney (HEK) cells through the transfection of three vector plasmids, as previously described (Rossi et al., 2014). The culture supernatant contained the lentiviral particles of interest, as well as cell debris and plasmid contaminants possibly able to activate TLR3, TLR7, or TLR9 (Alexopoulou et al., 2001; Beignon et al., 2005; Breckpot et al., 2010; Diebold et al., 2004; Pichlmair et al., 2007; Rossetti et al., 2011). Upon recognition of their respective PAMPs (pathogen-associated molecular patterns), TLRs recruit adaptor molecules that harbor the TIR (Toll/interleukin-1 receptor) domain, such as TRIF and MyD88, which are utilized by all TLRs with the exception of TLR3 (Kawai and Akira, 2010). These adaptors initiate signal cascades leading to the activation of interferon regulatory factors 3 and 7 (IRF3 and IRF7, respectively) (Thompson et al., 2011). We, thus, analyzed the CTL responses induced by IDLV-OVA in TLR-KO, MyD88-KO, and single and double IRF3 and IRF7-KO mice, in comparison with C57BL/6 mice (Figure 5). As expected, the absence of TLR9 or MyD88, but not of TLR3 or 7, fully abolished the CTL response induced by OVA plus CpG (Hemmi et al., 2000). These responses analyzed by an *in vivo* killing assay were also significantly reduced in IRF7- or IRF3/7-KO mice. In contrast, the OVA-specific CTL responses induced by IDLV-OVA and tested either by the *in vivo* killing assay or by ELISPOT were not decreased between the TLR3, TLR4, TLR7, TLR9, MyD88, IRF3, IRF7, and IRF3/7-KO mice and the C57BL/6 WT mice (Figures 5A–5H), showing that the induction of CTL responses by IDLV-OVA is fully independent of TLR and MyD88 and IRF signaling. However, a significant increase in these responses was observed in the IRF7 and

Figure 2. IDLVs Induce a Mild and Transient Maturation of Mouse DCs

C57BL/6 mice were injected i.v. with PBS, 5×10^6 TUs IDLV-OVA or CpG.

(A and B) The maturation of pDCs (left panels) and cDCs (right panels) was assessed from 6 h to 7 days after injection by monitoring the expression of CD80, CD86, and PDC-TREM by flow cytometry. The results are represented as histograms from one representative experiment (A) or expressed as the fold increase in MFI \pm SEM compared to pDCs or cDCs from PBS-injected mice 18 h after injection. The results represent the cumulative data from 25 to 30 mice from 9 independent experiments (B).

(C) The production of cytokines and chemokines in the sera of C57BL/6 mice injected with PBS, IDLV-OVA, or CpG was assessed up to 18 h after injection by Luminex MagPIX technology. The results are expressed in pg ml^{-1} and represent the cumulative data from 22 mice from 6 independent experiments. Statistical analysis was performed by unpaired Student's *t* test in comparison with the PBS-treated mice (ns $p > 0.05$, * $p < 0.05$, ** $p < 0.01$, *** $p < 0.001$, **** $p < 0.0001$). The statistical analysis in red corresponds to the statistics for CpG and in blue, to the statistics for IDLV-OVA compared to PBS-treated mice.

See also Figure S3.

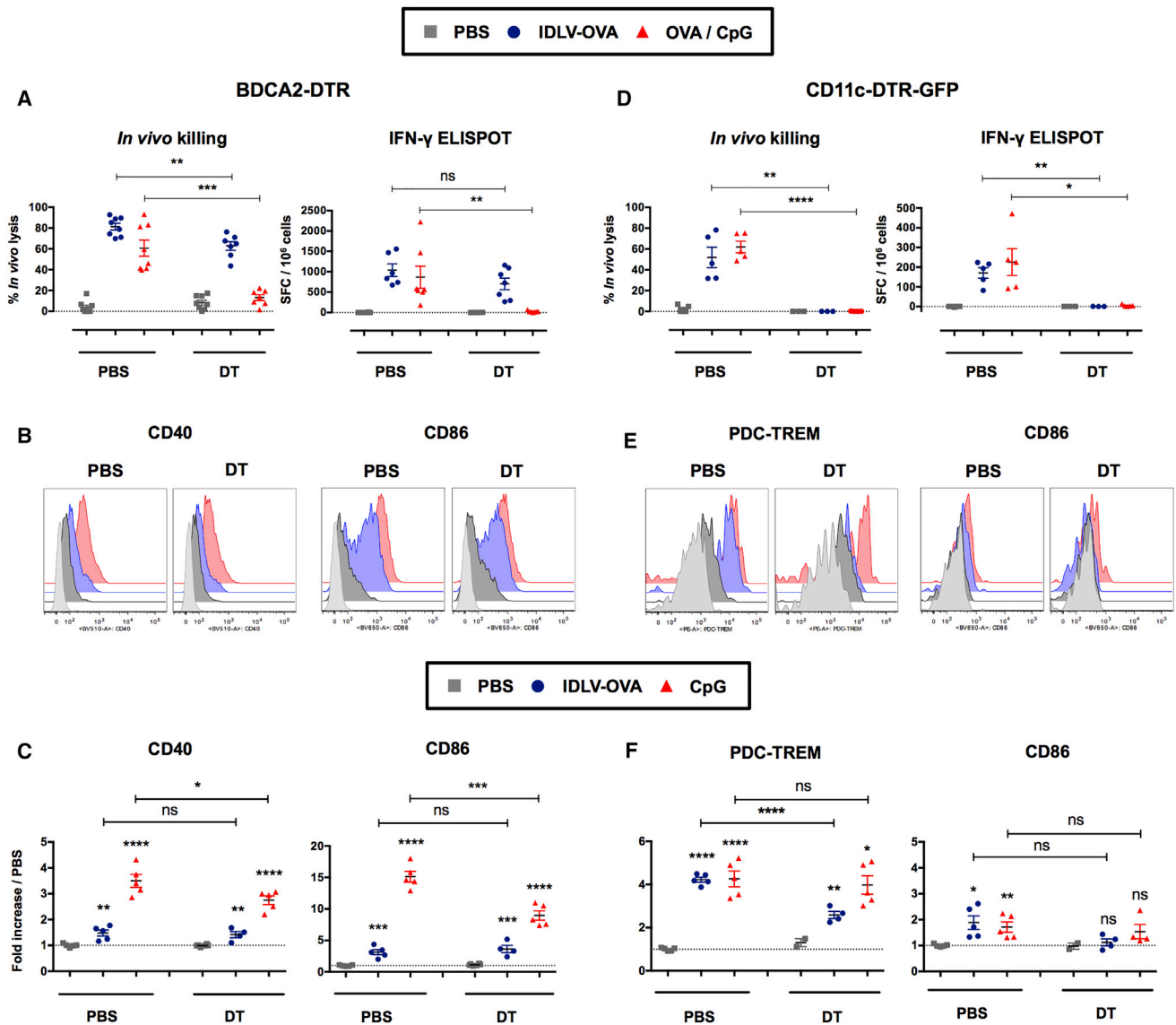


Figure 3. Conventional DCs Are Mandatory for the Induction of CTL Responses by IDLV-OVA

PBS- and DT-treated-BDCA2-DTR (A–C) and -CD11c-DTR → C57BL/6 chimeric mice (D–F) were injected i.v. with PBS, 10^6 (A and D), 5×10^6 TU IDLV-OVA (B, C, E, and F), OVA plus CpG (A and D), or CpG (B, C, E, and F). Seven days later, anti-OVA CTL responses were assessed by *in vivo* killing and IFN- γ ELISPOT assays (A and D). The results are expressed as the percentage of specific lysis for CTL activity and IFN- γ SFC per 10^6 splenocytes for ELISPOT. Each dot represents an individual mouse. The results represent the means \pm SEM of cumulative data from 6 to 8 mice collected from 3 independent experiments (A) or 3 to 5 mice from 2 independent experiments (D). Eighteen hours after injection, the expression of CD40 and CD86 by cDCs (B and C) and PDC-TREM and CD86 by pDCs (E and F) was assessed by flow cytometry. The results are represented as histograms from one representative experiment where isotype controls are indicated in light grey (B and E) or expressed as the fold-increase in MFI \pm SEM compared to cDCs or pDCs from PBS-injected mice (C and F). They represent the cumulative data from 4 to 6 mice (C) or 2 to 5 mice from 2 independent experiments (F). Statistical analysis was performed by unpaired Student's *t* test in comparison with the PBS-treated mice or between PBS- and DT-treated mice, as indicated by the horizontal bars (ns $p > 0.05$, * $p < 0.05$, ** $p < 0.01$, *** $p < 0.001$, **** $p < 0.0001$). See also [Figures S4](#) and [S5](#).

IRF3/7-KO mice, suggesting a negative regulatory role of IRF7 on the induction of immune responses by IDLVs.

The Induction of CTL Responses by IDLV-OVA Is Independent of the RIG-I and STING Pathways but Dependent on NF- κ B Signaling

Our results clearly show that cDCs are mandatory for the induction of CTL responses by IDLVs but that TLR signaling is not

involved in this process. To characterize the DC pathways activated by IDLVs, we analyzed the expression of 142 genes related to antiviral responses and NF- κ B signaling in splenic cDCs purified from mice injected with IDLVs ([Figures S7A](#) and [S7B](#)). Our results show that IDLVs induced a network of antiviral genes ([Figure 6A](#)). Four viral RNA pattern recognition genes were upregulated, of which RLRs such as *rig-1*, *Igp-2*, and *mda-5* increased by 5-, 4.2-, and 4-fold, respectively. The *pkri* gene,

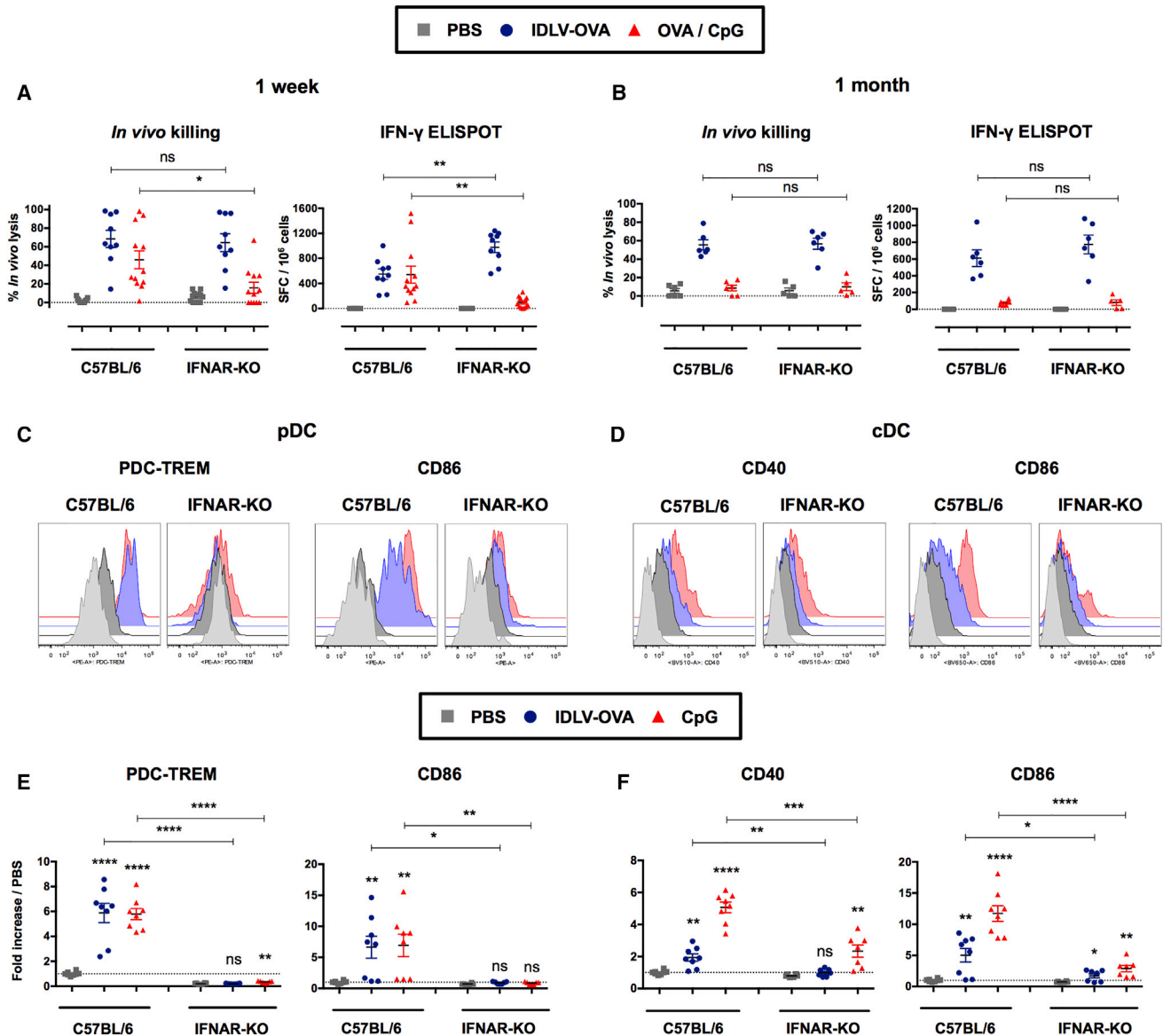


Figure 4. The Induction of CTL Responses by IDLV-OVA Does Not Require IFN-I Signaling

C57BL/6 and IFNAR-KO mice were injected i.v. with PBS, 10^6 TUs (A and B), 5×10^6 TUs (C–F) IDLV-OVA, OVA plus CpG (A and B), or CpG (C–F). Seven days (A) and 1 month (B) later, anti-OVA CTL responses were assessed by *in vivo* killing assay and IFN- γ ELISPOT. The results are expressed as the percentage of specific lysis for *in vivo* killing assay and IFN- γ SFC per 10^6 splenocytes for ELISPOT. Each dot represents an individual mouse. The results represent the means \pm SEM of cumulative data from 9 to 12 mice from 5 independent experiments (A) or 5 to 6 mice from 2 independent experiments (B). Eighteen hours after injection, the expression of PDC-TREM and CD86 by pDCs (C and E) and CD40 and CD86 by cDCs (D and F) was assessed by flow cytometry. The results are represented as histograms from one representative experiment where isotype controls are indicated in light grey (C and D) or expressed as the fold-increases in MFI \pm SEM compared to pDCs or cDCs from PBS-injected mice (E and F). They represent the cumulative data from 6 to 8 mice from 3 independent experiments. Statistical analysis was performed by unpaired Student's t test in comparison with the PBS-treated mice or between C57BL/6 and IFNAR-KO mice, as indicated by the horizontal bars (ns $p > 0.05$, * $p < 0.05$, ** $p < 0.01$, *** $p < 0.001$, **** $p < 0.0001$). See also Figure S6.

an enzyme activated by dsRNA, was upregulated 3.7-fold, reflecting the presence of viral RNA in the cytoplasm. The expression of two IFN signaling genes, *irf7* and *stat1*, also increased by 8.3- and 3.3-fold, respectively. Three antiviral IFN-stimulated genes (ISGs), *Isg15*, *Mx1*, and *Oas2*, were upregulated by 13.3-, 7.5-, and 5.6-fold, respectively, as well as the genes mediating antiviral immunity, such as the *Cxcl10* gene, which

increased by 21.3-fold. Thus, after sensing IDLV, DCs activate IFN signaling and antiviral response.

These results suggest that IDLVs, presumably through the ssRNA genome (Sakuma et al., 2012), activate the RIG-I pathway. Recently, 5'-triphosphate RNA (5'ppp-dsRNA) was demonstrated to be a selective ligand for RIG-I with the ability to induce strong CTL responses (Hornung et al., 2006;

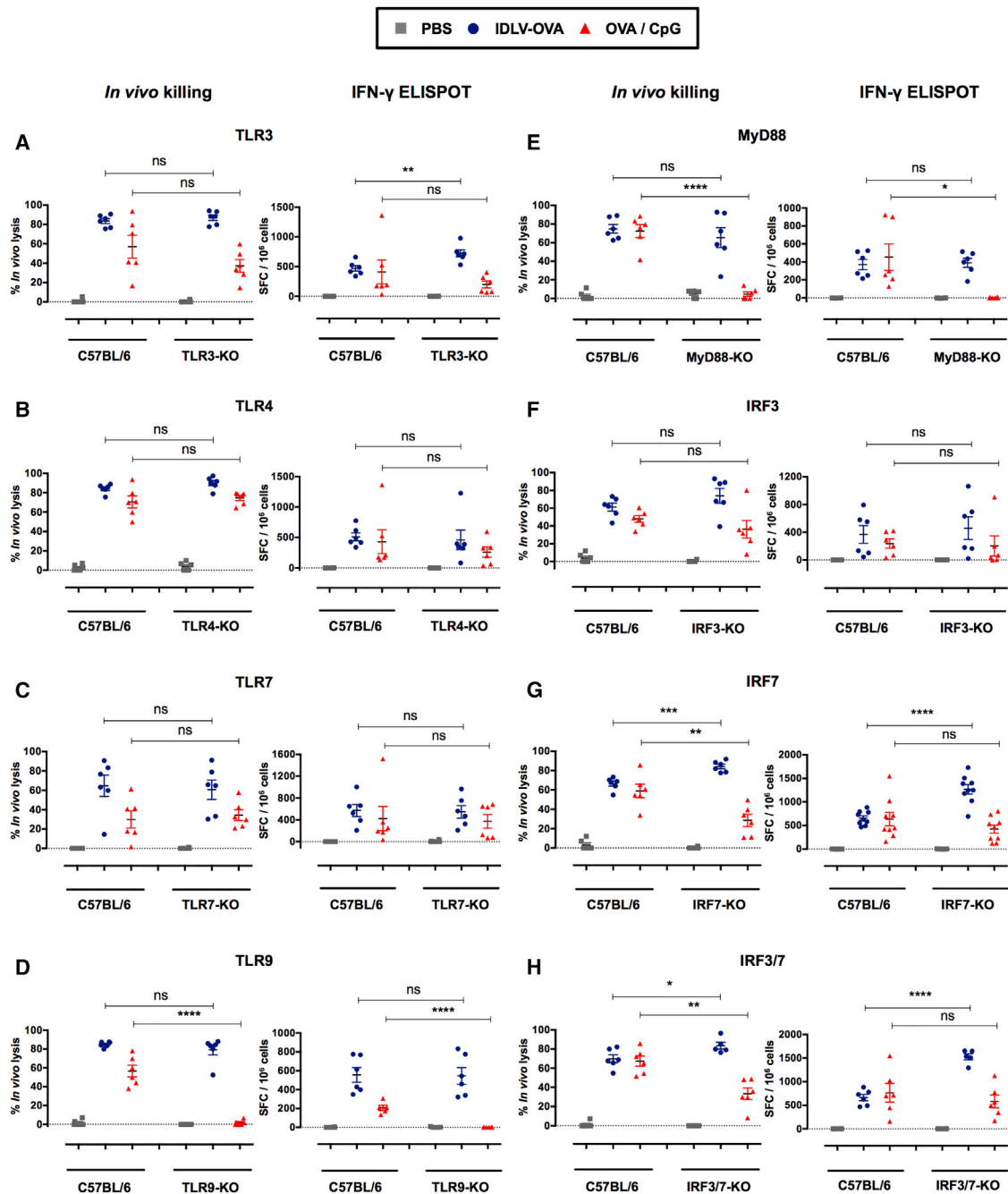


Figure 5. The Induction of CTL Responses by IDLV-OVA Is Independent of the TLR3, TLR4, TLR7, TLR9, MyD88, IRF3, and IRF7 Pathways C57BL/6, TLR3^{-/-} (A), TLR4^{-/-} (B), TLR7^{-/-} (C), TLR9^{-/-} (D), MyD88^{-/-} (E), IRF3^{-/-} (F), IRF7^{-/-} (G), and IRF3/7^{-/-} (H) mice were immunized i.v. with PBS, 10⁶ TUs IDLV-OVA or OVA plus CpG. Seven days later, anti-OVA CTL responses were assessed by *in vivo* killing assays (left panels) and IFN- γ ELISPOT assays (right panels). The results are expressed as the percentage of specific lysis for the *in vivo* killing assay and as the IFN- γ SFC per 10⁶ splenocytes for ELISPOT. Each dot represents an individual mouse. The results represent the means \pm SEM of cumulative data from 5 to 9 mice from 2 to 3 independent experiments. Statistical analysis was performed by an unpaired Student's *t* test in comparison with control C57BL/6 mice (ns *p* > 0.05, **p* < 0.05, ***p* < 0.01, ****p* < 0.001, *****p* < 0.0001).

Hochheiser et al., 2016). We, thus, compared the CTL responses induced by OVA in the presence of this RIG-I ligand and IDLV-OVA. One week after immunization, strong CTL responses were observed in mice immunized by IDLV-OVA or by OVA in

the presence of either 5'ppp-dsRNA or CpG, confirming the potent adjuvant property of this RIG-I ligand (Figure 6B). However, 1 month after immunization, these CTL responses vanished in the mice that received OVA with 5'ppp-dsRNA, whereas they

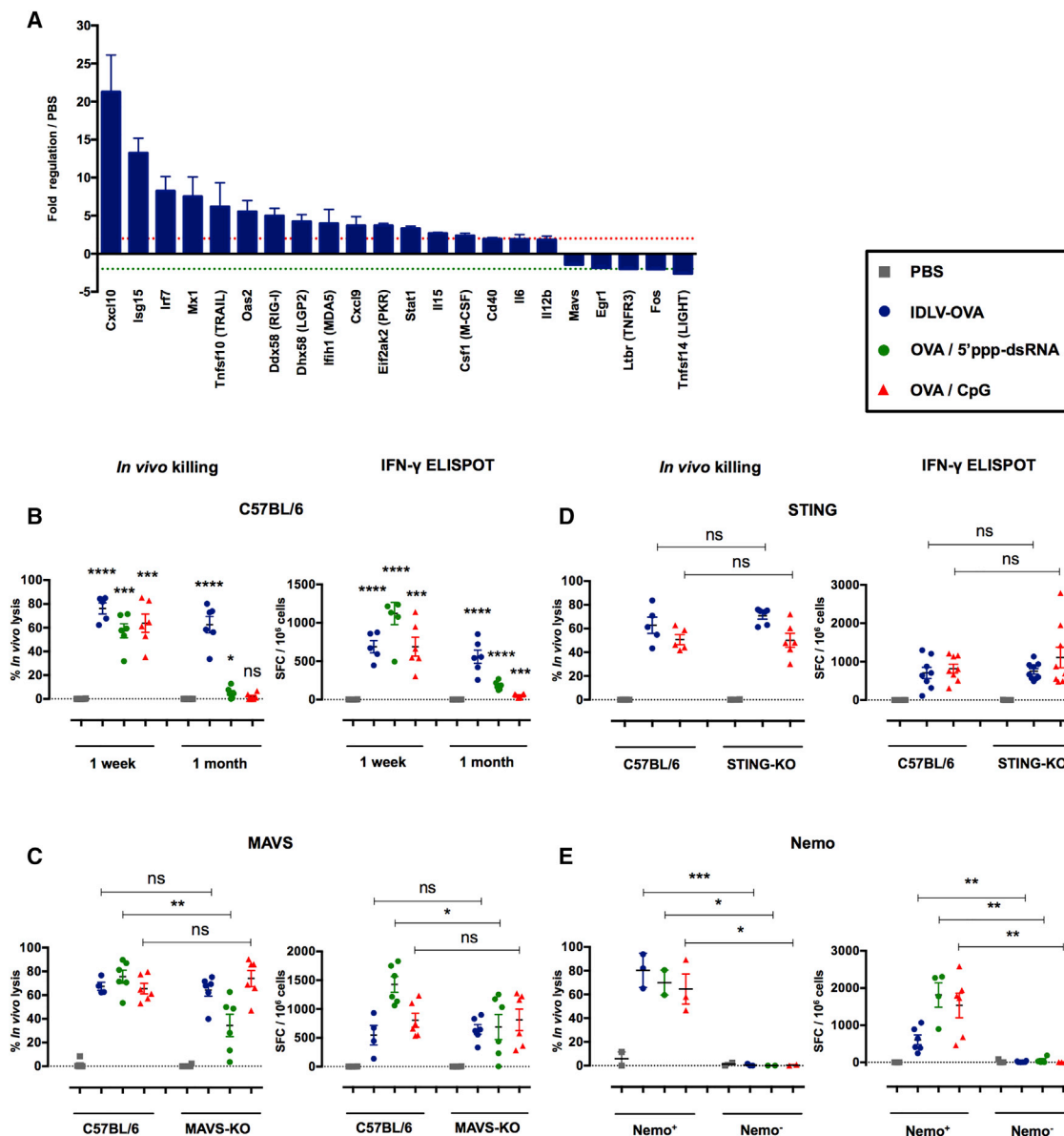


Figure 6. The Induction of CTL Responses by IDLV-OVA Is RIG-I and STING-Independent, but Depends upon the NF- κ B Pathway

(A) C57BL/6 mice were injected i.v. with PBS or 5×10^6 TUs IDLV-GFP. Four hours after injection, CD11c⁺ splenic cells were sorted, and the pathways involved in antiviral responses and NF- κ B signaling were analyzed using the RT² profiler PCR array. The results are expressed as the means \pm SEM of fold regulation compared to PBS-injected mice, and represent the cumulative data from two mice from two independent experiments. The green dashed line represents a threshold of two-fold downregulation and the red dashed line represents a threshold of two-fold upregulation.

(B–E) C57BL/6 (B), MAVS^{-/-} (C), STING^{-/-} (D), and CD11c-Cre x Nemo flox (E) mice were injected i.v. with PBS, 10^6 TUs IDLV-OVA, OVA plus 5'ppp-dsRNA, or OVA plus CpG. Seven days (B–E) or 1 month (B) later, anti-OVA CTL responses were assessed by an *in vivo* killing assay (left panels) and IFN- γ ELISPOT (right panels). The results are expressed as the percentage of specific lysis for the *in vivo* killing assay and IFN- γ SFC per 10^6 splenocytes for ELISPOT. Each dot represents an individual mouse. The results represent the means \pm SEM of cumulative data from 3 to 9 mice from 2 to 3 independent experiments (B–D) or 2 to 6 mice from 2 independent experiments (E). Nemo⁺ mice were born from the crossing of CD11c-Cre littermate nontransgenic mice and Nemo flox mice. In contrast, Nemo⁻ mice were born from the crossing of CD11c-Cre transgenic mice and Nemo flox mice. Statistical analysis was performed by unpaired Student's t test in comparison with PBS-treated mice or between control and deficient mice, as indicated by the horizontal bars (ns $p > 0.05$, * $p < 0.05$, ** $p < 0.01$, *** $p < 0.001$, **** $p < 0.0001$).

See also Figures S7, S8, and S9.

persisted in mice immunized with IDLV-OVA. This observation strongly suggests that the activation of the RIG-I pathway was not responsible for the persistence of these responses. To

confirm this conclusion, we next analyzed the CTL responses induced by IDLV-OVA in mice deficient in mitochondrial antiviral-signaling protein (MAVS), the common adaptor of RIG-I or

MDA5 (Seth et al., 2005), in comparison with C57BL/6 mice. As expected, the CTL responses induced by OVA in the presence of 5'ppp-dsRNA were strongly reduced in MAVS-KO mice, whereas they were not affected in mice immunized by IDLV-OVA or OVA plus CpG (Figure 6C), confirming the lack of contribution of the RIG-I pathway in their induction. It was recently shown that the STING-cGAS pathway is activated through genomic DNA encapsulated into LV virion preparation (Kim et al., 2017). However, strong CTL responses were induced by IDLV-OVA in STING-KO mice (Figure 6D), demonstrating the lack of involvement of STING signaling in the induction of CTL responses by our IDLV preparations. Finally, to investigate the role of NF- κ B in the induction of CTL responses by IDLV-OVA, we used Nemo flox transgenic mice with loxP sites, which were crossed with CD11c-Cre transgenic mice, resulting in the deletion of Nemo in CD11c⁺ cells. Indeed, Nemo is a protein necessary for the activation of NF- κ B signaling (Israël, 2010), whereas CD11c⁺ DCs are mandatory for the induction of CTL responses by IDLV-OVA. As shown in Figure 6E, the absence of Nemo in CD11c⁺ cells fully abolished the capacity of IDLV-OVA, OVA plus CpG, and OVA plus 5'ppp-dsRNA to stimulate CTL responses, clearly demonstrating that the induction of these responses is fully dependent on NF- κ B signaling.

To further characterize the NF- κ B pathway involved in the induction of CD8⁺ T cell responses by IDLV, we then performed a transcriptomic analysis of more than 750 genes expressed by cDCs following immunization with IDLV-OVA or CpG/OVA (Figures S8 and S9) by using the Nanostring technology. The hierarchical heatmap clustering analysis showed that cDCs from IDLV-OVA immunized mice exhibited a low transcriptional gene modulation compared to cDCs from CpG/OVA immunized mice (Figure S8A), confirming that IDLV induce a mild innate response. The analysis of the genes that were significantly induced or inhibited by cDCs from IDLV-OVA immunized mice compared to PBS-injected mice (Figure S8B) confirmed that cDCs were activated in mice immunized by IDLV-OVA, inducing the upregulation of antiviral genes. Furthermore, the analysis of the expression of cytokines and cytokine receptor genes (Figure S9A) confirmed that IDLV induced a weak cytokine production, as already shown by the quantification of cytokines and chemokines in the sera of immunized mice. These results also suggest that DCs could be the cells responsible for the production of IL-18 but not of IL-5. This analysis also showed that TRAF2/6 and RelA/B were upregulated in mice immunized with IDLV-OVA (Figure S9B), strongly suggesting that IDLV activates the canonical NF- κ B – Rel pathway. Furthermore, the downregulation of IL-1 β and the upregulation of TNF suggest that the activation of the NF- κ B – Rel pathway could be linked to TNF signaling.

The Long-Lasting CTL Responses Induced by IDLV-OVA Are Correlated with the Persistence of the Transgene in the Spleen and the Liver of Immunized Mice

These results do not identify a specific activation pathway involved in the induction of the CD8⁺ T cell response by IDLV-OVA that could explain the persistence of the CTL response induced by this vector. We, thus, tested whether this persistence could be due to a prolonged antigen expression in immunized mice. C57BL/6 mice were injected with IDLV-OVA, and the pres-

ence of the transgene was evaluated by PCR in the spleen (Figure 7A) and liver (Figure 7B) tissues of the vaccinated mice up to 3 months after injection. All DNA samples were subjected to glyceraldehyde 3-phosphate dehydrogenase (G3PDH) amplification to control for the DNA integrity (Figures 7A and 7B, bottom panels). The OVA transgene was still detectable in the spleen and/or the liver of all immunized mice 1 month after vaccination and in 50% of vaccinated mice up to 3 months after injection (after 2 months: 2/4 in spleen [lanes 1 and 3], and 1/4 in liver [lane 3]; and after 3 months: 1/4 in spleen [lane 2] and 1/4 in liver [lane 1]) (Figures 7A and 7B, top panels).

The long-term persistence of the transgene in immunized mice cannot be due to the integration of the vector, because we did not find any evidence of its integration (Figures 7C and 7D) 1 month after the injection of IDLV-OVA. This was in contrast to the DNA extracted from B16F10 cells infected with the integrase-competent LV expressing OVA, which was used as a positive control of vector integration.

These data demonstrate that despite the lack of integration, IDLV-OVA persists in the spleen and the liver of immunized mice, suggesting a long-term expression of the OVA antigen, which could be responsible for the persistence of the CTL responses.

DISCUSSION

In the present study, we evaluated the mechanisms underlying the strong effector memory CTL response, which persists up to 6 months after a single immunization, with an integrase-deficient lentiviral vector without adjuvant. The induction of these responses is fully dependent on cDCs, although IDLVs induce mild and transient innate responses, characterized by low levels of inflammatory cytokines and chemokines and weak DC maturation. The activation of efficient immune responses by IDLVs does not require the IFN-I, TLR and MyD88, IRF, RIG-I, and STING pathways but is fully dependent upon NF- κ B signaling in CD11c⁺ cells. Moreover, we demonstrate that despite their lack of integration, IDLV-OVA persist up to 3 months in the spleen and the liver of intravenously vaccinated mice, in correlation with their capacity to induce long-lasting immune responses and protective anti-tumoral immunity.

We first analyzed whether the capacity of IDLVs to induce strong CTL responses is due to the stimulation of sustained innate responses, leading to DC activation and to the production of inflammatory cytokines and chemokines. Indeed, both cDCs and pDCs were activated following immunization by IDLVs, although cDCs were the only DCs required for the induction of CD8⁺ T cell responses. However, compared to CpG/OVA, IDLVs induced a mild and transient activation of cDCs, which was detectable only after the administration of high doses of IDLV-OVA. Interestingly, lower doses of IDLV-OVA were still capable of promoting the induction of strong CTL responses but could not induce a detectable maturation of DCs. Thus, the magnitude and the duration of CTL responses induced by IDLV-OVA, compared to CpG/OVA, were not correlated with the level of innate responses induced by these vaccines.

Remarkably, IDLVs in contrast to CpG induced a very low level of inflammatory cytokines and chemokines. It has been shown that IFN-I and/or IL-12 are required for the expansion of highly

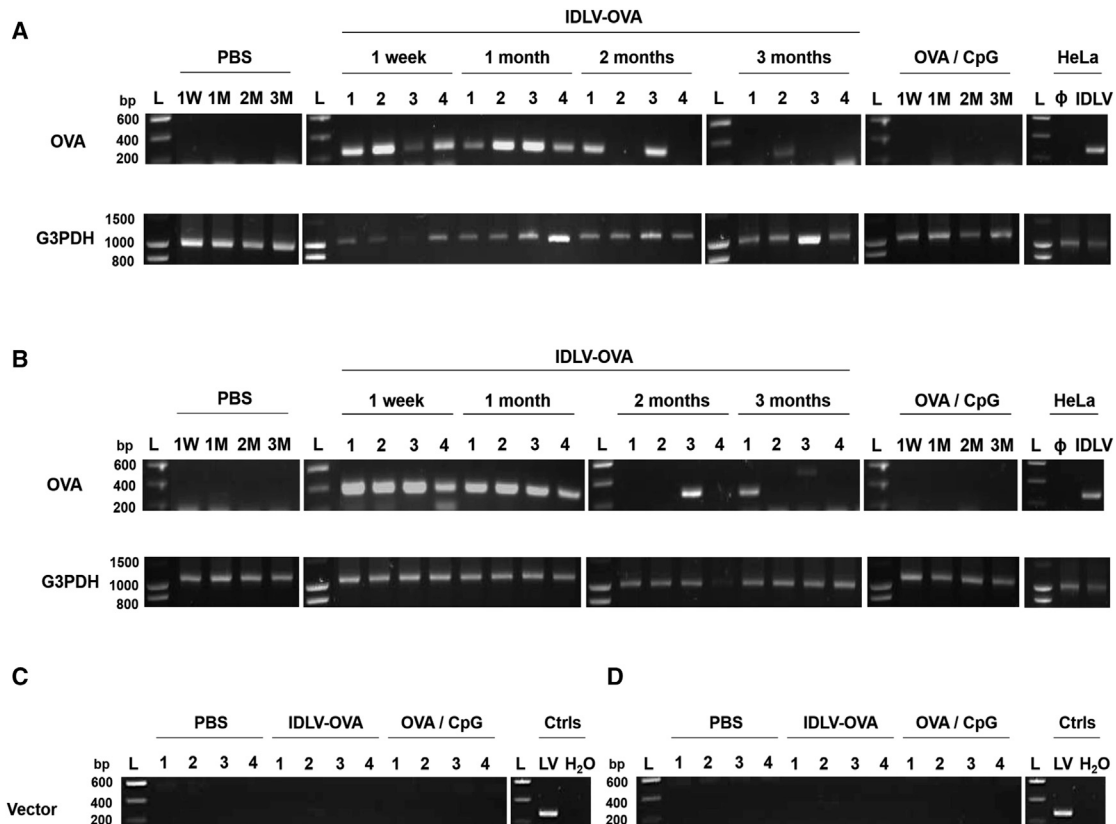


Figure 7. The Long-Term Persistence of the CTL Responses Induced by IDLV-OVA Correlates with the Persistence of the Transgene in the Spleen and the Liver of Vaccinated Mice

C57BL/6 mice were injected i.v. with PBS, 10^6 TUs IDLV-OVA or OVA plus CpG.

(A and B) One week or one, two or three months later, spleens (A) and livers (B) were harvested. DNA was extracted and amplified using the corresponding primer pair. At each time point, 4 mice were included for the IDLV-OVA treatment, whereas 1 mouse per time point is shown for the PBS and OVA plus CpG groups. The presence of the OVA transgene (top panels) and the G3PDH (DNA integrity, bottom panels) was evaluated by PCR.

(C and D) 1 month after injection, spleens (C) and livers (D) were harvested, and DNA was extracted and amplified using the corresponding primer pair to evaluate vector integration. At each time point, 4 mice were included per treatment. The positive and negative controls used to detect the presence of the OVA transgene were subjected to DNA extraction from HeLa cells, transduced or not (ϕ) with IDLV-OVA (IDLV). G3PDH, glyceraldehyde 3-phosphate dehydrogenase; L, ladder; Ctrls, controls performed on DNA extracted from B16F10 cells infected with the integrase competent lentiviral vector (LV) expressing OVA and with a PCR performed with H₂O.

cytolytic effector CD8⁺ T cells. Indeed, T cells exposed to high levels of IL-2 preferentially attain a terminally differentiated, short-lived effector phenotype. By contrast, the restriction of inflammatory conditions surrounding CD8⁺ T cells allows the formation of long-lived memory populations (Cox et al., 2013). These data are in agreement with our observations that CpG, which induces the secretion of IFN-I and IL-12p70, allows the expansion of short-lived effector CD8⁺ T cells, while the lack of production of IFN-I and IL-12p70 and the low secretion of IL-2 following IDLV-OVA immunization correlate with the induction of long-lasting CD8⁺ T cell responses. Upon IDLV-OVA treatment, only IL-5 and IL-18 were detectable. These cytokines have been shown to be required for an optimal CTL response and are associated with IFN- γ production by effector and memory CD8⁺ T cells (Apostolopoulos et al., 2000; Cox et al., 2013), strongly suggesting that IL-5 and IL-18 are implicated in the induction of cytotoxic responses by IDLVs.

One week after vaccination, OVA-specific CD8⁺ T cells induced by IDLV-OVA expressed a classical effector CTL phenotype (Wherry and Ahmed, 2004), similar to the OVA-specific CD8⁺ T cells induced by OVA plus CpG. However, the expression of CD27 and CD44 were significantly more upregulated in CTL cells induced by IDLV-OVA than after immunization with OVA plus CpG. The engagement of CD27 promotes the development of CTL effectors and the survival of TCR-activated T cells (Hendriks et al., 2003). It also regulates their expansion at the site of priming, maintenance at the effector site, contraction, memory formation, and secondary expansion. A major mechanism by which CD27 affects the T cell response is their protection from apoptosis. The analysis of gene expression showed that OVA-specific CD8⁺ T cells induced by IDLV-OVA downregulate genes involved in apoptosis (*Casp3*) (Porter and Jänicke, 1999) and in T cell exhaustion (*Havcr2*, *Lag3*, and *Tigit*) (Wherry and Kurachi, 2015) compared to OVA plus CpG. In

addition, several genes involved in the activation of T lymphocytes were downregulated (*Tnfrsf4*) (Watts, 2005), although others were upregulated (*Klrk1*) (Jamieson et al., 2002). Thus, it could be suggested that the strong activation of CTLs by OVA plus CpG is followed by the rapid exhaustion of CD8⁺ T cells and apoptosis. In contrast, CD8⁺ T cells induced by IDLV-OVA could be less activated, eventually due to the low innate responses induced by this vector compared to CpG. They are, therefore, less prone to cell death and exhaustion, leading to a longer survival.

IFN-I was shown to be important in the induction of CD8⁺ T cell responses, as confirmed previously for CpG/OVA (Hervas-Stubbs et al., 2014). In contrast, the present study demonstrates that the effector and memory T cell responses induced by IDLVs are totally independent of IFN-I signaling. However, cDC activation and maturation induced by IDLV-OVA were strongly reduced in the absence of IFN-I signaling. These results confirm that efficient CTL responses could be induced by IDLV-OVA, even with the low maturation of cDCs.

HIV-1 possesses an ssRNA genome (Sakuma et al., 2012) that could be directly detected into the cytosol by the RIG-I receptor or by TLR7 in the endocytic compartment (Pichlmair et al., 2006; Diebold et al., 2004). Through the action of the viral reverse transcriptase or RNA polymerase III, ssRNA is converted into dsDNA or dsRNA, which could be detected respectively into the cells by cytosolic DNA sensors that act upstream of STING (Gürtler and Bowie, 2013) or by TLR3 (Alexopoulou et al., 2001). In addition, tubovesicular structures containing nucleic acids present in the vector preparation could also stimulate TLR9 (Pichlmair et al., 2007). Several studies have shown the involvement of both TLR (TLR3, TLR7, and TLR9) and non-TLR-mediated mechanisms involving LV proviral DNA in the sensing of LVs (Beignon et al., 2005; Breckpot et al., 2010; Rossetti et al., 2011; Agudo et al., 2012). NF- κ B signaling could be engaged by IDLV-OVA, as the activation of RLR signaling leads to its activation (Nan et al., 2014). Moreover, NF- κ B could also be activated by the dsRNA-dependent protein kinase R (PKR) (Gil et al., 2000), which is upregulated upon IDLV treatment. In agreement with these hypotheses, the absence of Nemo in CD11c⁺ cells fully abolished the capacity of IDLV-OVA to stimulate CTL responses, clearly demonstrating that the induction of these responses was fully dependent upon NF- κ B signaling in DCs. In agreement with these findings, the transcriptomic analysis of genes expressed by cDCs after immunization with IDLV-OVA demonstrated that IDLV activated the canonical NF- κ B – Rel pathway. Altogether, these data suggest the presence of IDLV RNA in the cytoplasm of immunized mice, which could be detected by either RIG-I or PKR leading to NF- κ B activation. However, mice deficient in TLR and MyD88, IRF, RIG-I, or melanoma differentiation-associated protein 5 (MDA5) were fully capable of developing strong CTL responses after IDLV-OVA immunization. These results suggest that IDLVs are not recognized by these sensors. Alternatively, it could be proposed that IDLVs can signal through several of these pathways, which could compensate for an absence in one of them.

In agreement with our results, it was recently shown that the activation of DCs by LVs is independent of MyD88, toll-interleukin-1 receptor-domain-containing adapter-inducing inter-

feron- β (TRIF), and MAVS, ruling out the involvement of TLR or RLR signaling. However, this study also concluded that two different pathways could contribute to the *in vitro* activation of mouse bone marrow-derived DCs (BMDCs) and human monocytic DCs by LVs (Kim et al., 2017). LVs could induce cell activation either following envelope-mediated viral fusion in a PI3K-dependent process or by the cellular DNA packaged in these LV preparations, which stimulates the STING-cGAS pathway. However, the requirement of each of these processes in the *in vivo* activation of DCs was not clearly established. Indeed, although CD8⁺ T cell responses induced by LVs were reduced in mice deficient for STING and cGAS, the activation of the DCs of these immunized mice was not analyzed. In contrast to this study, our present data clearly show that IDLVs induce efficient CTL responses in STING-deficient mice compared to C57BL/6 mice, thus demonstrating that STING is not involved in the induction of CD8⁺ T cell responses by IDLV-OVA. The discrepancy of our results with Kim's study (Kim et al., 2017) could be explained by the mode of IDLV preparation or by the route of immunization used. In Kim's study, the STING-cGAS pathway was activated not by the virion itself but by the human genomic DNA packaged during the preparation of LVs. This contaminant human DNA could, thus, play an important role in the induction of immune responses by the LVs used in that study.

Finally, we demonstrate that despite the lack of integration of IDLV-OVA, the OVA transgene was detectable in the spleen and the liver of vaccinated mice up to 3 months after a single intravenous injection. Interestingly, it was previously demonstrated that IDLVs could be detected at the injection site up to 3 months after intramuscular administration (Negri et al., 2007; Karwacz et al., 2009). Altogether, these data suggest that the antigen can be expressed during several months after immunization, which could explain how high frequencies of antigen-specific CD8⁺ T cells are maintained following immunization with lentivirus (He et al., 2005; Kimura et al., 2007). The expression of the transgene delivered by IDLVs persists in transduced human macrophages but is rapidly lost in dividing cells (Gillim-Ross et al., 2005). Macrophages are long-lived cells (Takahashi, 2001) and, thus, can stimulate naive CD8⁺ T cells to proliferate and differentiate into memory T cells (Pozzi et al., 2005). Recent studies have shown that DCs retain their dividing abilities and could maintain the expression of antigens in their progeny directly through successive cell divisions (Diao et al., 2007).

In conclusion, the present study demonstrates that a single immunization with low doses of IDLVs induce strong CTL responses that were fully dependent upon NF- κ B signaling in CD11c⁺ DCs. Despite their lack of integration, the transgene persists in the spleen and the liver of vaccinated mice, leading to a long-lasting memory CTL response associated with protective antitumor immunity. Thus, we identify the persistence of the vector as an important parameter for the induction of efficient adaptive immune responses. In addition, our study also shows that sustained inflammatory responses are not required for the optimal induction of the immune response. This study highlights the improved safety and efficacy of IDLVs and provides important features to be considered for the development of new vaccine strategies.

STAR★METHODS

Detailed methods are provided in the online version of this paper and include the following:

- **KEY RESOURCES TABLE**
- **CONTACT FOR REAGENT AND RESOURCE SHARING**
- **EXPERIMENTAL MODEL AND SUBJECT DETAILS**
 - *In vivo* animal studies
 - Cell lines
- **METHOD DETAILS**
 - Reagents
 - Lentiviral vector production
 - Coding sequence of the OVA protein
 - Flow cytometry analysis
 - Analysis of cytokine and chemokine production
 - *In vivo* killing assay
 - IFN- γ ELISPOT assay
 - PCR arrays
 - Genotyping of mice with NEMO-deficient CD11c⁺ cells
 - Transcriptomic analysis
 - OVA transgene and vector integration analysis
- **QUANTIFICATION AND STATISTICAL ANALYSIS**

SUPPLEMENTAL INFORMATION

Supplemental Information includes nine figures and one table and can be found with this article online at <https://doi.org/10.1016/j.celrep.2019.01.025>.

ACKNOWLEDGMENTS

We thank Molly Ingersoll, Hélène Saklani, Noëlle Doyen, Martine Fanton, and Christian Vossnerich for providing the TLR3-, TLR7-, TLR9-, IRF3-, IRF7-, and IRF3/7-deficient mice and Nemo flox transgenic mice. We also thank Catherine Fitting, Martina Borghi, Alessandra Gallinaro, and Nathalie Nadeau for their help in the Luminex experiments, the titration of IDLV batches, and the migration of PCR products, respectively. This work was supported by the ADITEC project, which received funding from the European Union's Seventh Programme for research, technological development and demonstration under grant agreement number 280873.

AUTHOR CONTRIBUTIONS

C.C. designed and performed the experiments, analyzed the results, and wrote the manuscript; D.N., T.F., P.R., and V.M. designed and performed some of the experiments and analyzed the results; M.O. designed and performed the FACS sorting experiments and provided help with the FACS gating strategies, macroarray experiments, and mouse breeding; A.C. and D.N. provided the plasmids necessary to produce IDLV-OVA and IDLV-GFP and the DNA extracted from B16F10 cells transduced with LV-OVA and critically edited the manuscript; R.W. provided help for the migration of PCR products; S.F. produced IDLV-OVA and IDLV-GFP; C.L. and G.D. conceived and supervised the study, designed the experiments, analyzed and discussed the data, and wrote the manuscript; and G.D. performed several experiments.

DECLARATION OF INTERESTS

The authors declare no competing interests.

Received: June 6, 2018

Revised: November 22, 2018

Accepted: January 7, 2019

Published: January 29, 2019

REFERENCES

- Agudo, J., Ruzo, A., Kitur, K., Sachidanandam, R., Blander, J.M., and Brown, B.D. (2012). A TLR and non-TLR mediated innate response to lentiviruses restricts hepatocyte entry and can be ameliorated by pharmacological blockade. *Mol. Ther.* *20*, 2257–2267.
- Aiuti, A., Biasco, L., Scaramuzza, S., Ferrua, F., Cicalese, M.P., Baricordi, C., Dionisio, F., Calabria, A., Giannelli, S., Castiello, M.C., et al. (2013). Lentiviral hematopoietic stem cell gene therapy in patients with Wiskott-Aldrich syndrome. *Science* *341*, 1233151.
- Alexopoulou, L., Holt, A.C., Medzhitov, R., and Flavell, R.A. (2001). Recognition of double-stranded RNA and activation of NF- κ B by Toll-like receptor 3. *Nature* *413*, 732–738.
- Apostolopoulos, V., McKenzie, I.F., Lees, C., Matthaei, K.I., and Young, I.G. (2000). A role for IL-5 in the induction of cytotoxic T lymphocytes in vivo. *Eur. J. Immunol.* *30*, 1733–1739.
- Beignon, A.S., McKenna, K., Skoberne, M., Manches, O., DaSilva, I., Kavanagh, D.G., Larsson, M., Gorelick, R.J., Lifson, J.D., and Bhardwaj, N. (2005). Endocytosis of HIV-1 activates plasmacytoid dendritic cells via Toll-like receptor-viral RNA interactions. *J. Clin. Invest.* *115*, 3265–3275.
- Beignon, A.S., Mollier, K., Liard, C., Coutant, F., Munier, S., Rivière, J., Souque, P., and Charneau, P. (2009). Lentiviral vector-based prime/boost vaccination against AIDS: pilot study shows protection against Simian immunodeficiency virus SIVmac251 challenge in macaques. *J. Virol.* *83*, 10963–10974.
- Biffi, A., Montini, E., Lorioli, L., Cesani, M., Fumagalli, F., Plati, T., Baldoli, C., Martino, S., Calabria, A., Canale, S., et al. (2013). Lentiviral hematopoietic stem cell gene therapy benefits metachromatic leukodystrophy. *Science* *341*, 1233158.
- Bonifaz, L., Bonnyay, D., Mahnke, K., Rivera, M., Nussenzweig, M.C., and Steinman, R.M. (2002). Efficient targeting of protein antigen to the dendritic cell receptor DEC-205 in the steady state leads to antigen presentation on major histocompatibility complex class I products and peripheral CD8+ T cell tolerance. *J. Exp. Med.* *196*, 1627–1638.
- Breckpot, K., Escors, D., Arce, F., Lopes, L., Karwacz, K., Van Lint, S., Keyaerts, M., and Collins, M. (2010). HIV-1 lentiviral vector immunogenicity is mediated by Toll-like receptor 3 (TLR3) and TLR7. *J. Virol.* *84*, 5627–5636.
- Cartier, N., Hacein-Bey-Abina, S., Bartholomae, C.C., Veres, G., Schmidt, M., Kutschera, I., Vidaud, M., Abel, U., Dal-Cortivo, L., Caccavelli, L., et al. (2009). Hematopoietic stem cell gene therapy with a lentiviral vector in X-linked adrenoleukodystrophy. *Science* *326*, 818–823.
- Caton, M.L., Smith-Raska, M.R., and Reizis, B. (2007). Notch-RBP-J signaling controls the homeostasis of CD8- dendritic cells in the spleen. *J. Exp. Med.* *204*, 1653–1664.
- Chinnasamy, N., Chinnasamy, D., Toso, J.F., Lapointe, R., Candotti, F., Morgan, R.A., and Hwu, P. (2000). Efficient gene transfer to human peripheral blood monocyte-derived dendritic cells using human immunodeficiency virus type 1-based lentiviral vectors. *Hum. Gene Ther.* *11*, 1901–1909.
- Cox, M.A., Kahan, S.M., and Zajac, A.J. (2013). Anti-viral CD8 T cells and the cytokines that they love. *Virology* *435*, 157–169.
- Diao, J., Winter, E., Chen, W., Xu, F., and Catral, M.S. (2007). Antigen transmission by replicating antigen-bearing dendritic cells. *J. Immunol.* *179*, 2713–2721.
- Diebold, S.S., Kaisho, T., Hemmi, H., Akira, S., and Reis e Sousa, C. (2004). Innate antiviral responses by means of TLR7-mediated recognition of single-stranded RNA. *Science* *303*, 1529–1531.
- Esslinger, C., Romero, P., and MacDonald, H.R. (2002). Efficient transduction of dendritic cells and induction of a T-cell response by third-generation lentivectors. *Hum. Gene Ther.* *13*, 1091–1100.
- Fritz, J.H., Ferrero, R.L., Philpott, D.J., and Girardin, S.E. (2006). Nod-like proteins in immunity, inflammation and disease. *Nat. Immunol.* *7*, 1250–1257.
- Geijtenbeek, T.B., and Gringhuis, S.I. (2009). Signalling through C-type lectin receptors: shaping immune responses. *Nat. Rev. Immunol.* *9*, 465–479.

- Gil, J., Alcamí, J., and Esteban, M. (2000). Activation of NF-kappa B by the dsRNA-dependent protein kinase, PKR involves the I kappa B kinase complex. *Oncogene* *19*, 1369–1378.
- Gillim-Ross, L., Cara, A., and Klotman, M.E. (2005). HIV-1 extrachromosomal 2-LTR circular DNA is long-lived in human macrophages. *Viral Immunol.* *18*, 190–196.
- Grasso, F., Negri, D.R., Mochi, S., Rossi, A., Cesolini, A., Giovannelli, A., Chiantore, M.V., Leone, P., Giorgi, C., and Cara, A. (2013). Successful therapeutic vaccination with integrase defective lentiviral vector expressing nononcogenic human papillomavirus E7 protein. *Int. J. Cancer* *132*, 335–344.
- Gürtler, C., and Bowie, A.G. (2013). Innate immune detection of microbial nucleic acids. *Trends Microbiol.* *21*, 413–420.
- Hacein-Bey-Abina, S., Von Kalle, C., Schmidt, M., McCormack, M.P., Wulfraat, N., Leboulch, P., Lim, A., Osborne, C.S., Pawliuk, R., Morillon, E., et al. (2003). LMO2-associated clonal T cell proliferation in two patients after gene therapy for SCID-X1. *Science* *302*, 415–419.
- Hacein-Bey-Abina, S., Hauer, J., Lim, A., Picard, C., Wang, G.P., Berry, C.C., Martinache, C., Rieux-Laucat, F., Latour, S., Belohradsky, B.H., et al. (2010). Efficacy of gene therapy for X-linked severe combined immunodeficiency. *N. Engl. J. Med.* *363*, 355–364.
- He, Y., Zhang, J., Mi, Z., Robbins, P., and Faló, L.D., Jr. (2005). Immunization with lentiviral vector-transduced dendritic cells induces strong and long-lasting T cell responses and therapeutic immunity. *J. Immunol.* *174*, 3808–3817.
- Hemmi, H., Takeuchi, O., Kawai, T., Kaisho, T., Sato, S., Sanjo, H., Matsumoto, M., Hoshino, K., Wagner, H., Takeda, K., and Akira, S. (2000). A Toll-like receptor recognizes bacterial DNA. *Nature* *408*, 740–745.
- Hemmi, H., Kaisho, T., Takeuchi, O., Sato, S., Sanjo, H., Hoshino, K., Horiuchi, T., Tomizawa, H., Takeda, K., and Akira, S. (2002). Small anti-viral compounds activate immune cells via the TLR7/MyD88-dependent signaling pathway. *Nat. Immunol.* *3*, 196–200.
- Hendriks, J., Xiao, Y., and Borst, J. (2003). CD27 promotes survival of activated T cells and complements CD28 in generation and establishment of the effector T cell pool. *J. Exp. Med.* *198*, 1369–1380.
- Hervas-Stubbs, S., Olivier, A., Boisgerault, F., Thieblemont, N., and Leclerc, C. (2007). TLR3 ligand stimulates fully functional memory CD8+ T cells in the absence of CD4+ T-cell help. *Blood* *109*, 5318–5326.
- Hervas-Stubbs, S., Riezu-Boj, J.I., Mancheño, U., Rueda, P., Lopez, L., Alignani, D., Rodríguez-García, E., Thieblemont, N., and Leclerc, C. (2014). Conventional but not plasmacytoid dendritic cells foster the systemic virus-induced type I IFN response needed for efficient CD8 T cell priming. *J. Immunol.* *193*, 1151–1161.
- Hochheiser, K., Klein, M., Gottschalk, C., Hoss, F., Scheu, S., Coch, C., Hartmann, G., and Kurts, C. (2016). Cutting edge: the RIG-I ligand 3pRNA potently improves CTL cross-priming and facilitates antiviral vaccination. *J. Immunol.* *196*, 2439–2443.
- Honda, K., Yanai, H., Negishi, H., Asagiri, M., Sato, M., Mizutani, T., Shimada, N., Ohba, Y., Takaoka, A., Yoshida, N., and Taniguchi, T. (2005). IRF-7 is the master regulator of type-I interferon-dependent immune responses. *Nature* *434*, 772–777.
- Hornung, V., Ellegast, J., Kim, S., Brzózka, K., Jung, A., Kato, H., Poeck, H., Akira, S., Conzelmann, K.K., Schlee, M., et al. (2006). 5'-Triphosphate RNA is the ligand for RIG-I. *Science* *314*, 994–997.
- Hoshino, K., Takeuchi, O., Kawai, T., Sanjo, H., Ogawa, T., Takeda, Y., Takeda, K., and Akira, S. (1999). Cutting edge: Toll-like receptor 4 (TLR4)-deficient mice are hyporesponsive to lipopolysaccharide: evidence for TLR4 as the Lps gene product. *J. Immunol.* *162*, 3749–3752.
- Israël, A. (2010). The IKK complex, a central regulator of NF-kappaB activation. *Cold Spring Harb. Perspect. Biol.* *2*, a000158.
- Jamieson, A.M., Diefenbach, A., McMahon, C.W., Xiong, N., Carlyle, J.R., and Raulet, D.H. (2002). The role of the NKG2D immunoreceptor in immune cell activation and natural killing. *Immunity* *17*, 19–29.
- Jung, S., Unutmaz, D., Wong, P., Sano, G., De los Santos, K., Sparwasser, T., Wu, S., Vuthoori, S., Ko, K., Zavala, F., et al. (2002). In vivo depletion of CD11c+
- dendritic cells abrogates priming of CD8+ T cells by exogenous cell-associated antigens. *Immunity* *17*, 211–220.
- Karwacz, K., Mukherjee, S., Apolonia, L., Blundell, M.P., Bouma, G., Escors, D., Collins, M.K., and Thrasher, A.J. (2009). Nonintegrating lentiviral vaccines stimulate prolonged T-cell and antibody responses and are effective in tumor therapy. *J. Virol.* *83*, 3094–3103.
- Kawai, T., and Akira, S. (2010). The role of pattern-recognition receptors in innate immunity: update on Toll-like receptors. *Nat. Immunol.* *11*, 373–384.
- Kawai, T., Adachi, O., Ogawa, T., Takeda, K., and Akira, S. (1999). Unresponsiveness of MyD88-deficient mice to endotoxin. *Immunity* *11*, 115–122.
- Kim, J.T., Liu, Y., Kulkarni, R.P., Lee, K.K., Dai, B., Lovely, G., Ouyang, Y., Wang, P., Yang, L., and Baltimore, D. (2017). Dendritic cell-targeted lentiviral vector immunization uses pseudotransduction and DNA-mediated STING and cGAS activation. *Sci. Immunol.* *2*, eaal1329.
- Kimura, T., Koya, R.C., Anselmi, L., Sternini, C., Wang, H.J., Comin-Anduix, B., Prins, R.M., Faure-Kumar, E., Rozengurt, N., Cui, Y., et al. (2007). Lentiviral vectors with CMV or MHCII promoters administered in vivo: immune reactivity versus persistence of expression. *Mol. Ther.* *15*, 1390–1399.
- Love, M.I., Huber, W., and Anders, S. (2014). Moderated estimation of fold change and dispersion for RNA-seq data with DESeq2. *Genome Biol.* *15*, 550.
- Müller, U., Steinhoff, U., Reis, L.F., Hemmi, S., Pavlovic, J., Zinkernagel, R.M., and Aguet, M. (1994). Functional role of type I and type II interferons in antiviral defense. *Science* *264*, 1918–1921.
- Nan, Y., Nan, G., and Zhang, Y.J. (2014). Interferon induction by RNA viruses and antagonism by viral pathogens. *Viruses* *6*, 4999–5027.
- Nayak, S., and Herzog, R.W. (2010). Progress and prospects: immune responses to viral vectors. *Gene Ther.* *17*, 295–304.
- Negri, D.R., Michelini, Z., Baroncelli, S., Spada, M., Vendetti, S., Buffa, V., Bona, R., Leone, P., Klotman, M.E., and Cara, A. (2007). Successful immunization with a single injection of non-integrating lentiviral vector. *Mol. Ther.* *15*, 1716–1723.
- Otto, P.K.D., Bitner, R., Huber, S., and Volkerding, K. (1998). Separate isolation of genomic DNA and total RNA from single samples using the SV total RNA isolation system. *Promega Notes* *69*, 19–24.
- Philippe, S., Sarkis, C., Barkats, M., Mammeri, H., Ladroue, C., Petit, C., Mallet, J., and Serguera, C. (2006). Lentiviral vectors with a defective integrase allow efficient and sustained transgene expression in vitro and in vivo. *Proc. Natl. Acad. Sci. USA* *103*, 17684–17689.
- Pichlmair, A., Schulz, O., Tan, C.P., Näsälund, T.I., Liljeström, P., Weber, F., and Reis e Sousa, C. (2006). RIG-I-mediated antiviral responses to single-stranded RNA bearing 5'-phosphates. *Science* *314*, 997–1001.
- Pichlmair, A., Diebold, S.S., Gschmeissner, S., Takeuchi, Y., Ikeda, Y., Collins, M.K., and Reis e Sousa, C. (2007). Tubulovesicular structures within vesicular stomatitis virus G protein-pseudotyped lentiviral vector preparations carry DNA and stimulate antiviral responses via Toll-like receptor 9. *J. Virol.* *81*, 539–547.
- Porter, A.G., and Jänicke, R.U. (1999). Emerging roles of caspase-3 in apoptosis. *Cell Death Differ.* *6*, 99–104.
- Pozzi, L.A., Maciaszek, J.W., and Rock, K.L. (2005). Both dendritic cells and macrophages can stimulate naive CD8 T cells in vivo to proliferate, develop effector function, and differentiate into memory cells. *J. Immunol.* *175*, 2071–2081.
- Probst, H.C., Lagnel, J., Kollias, G., and van den Broek, M. (2003). Inducible transgenic mice reveal resting dendritic cells as potent inducers of CD8+ T cell tolerance. *Immunity* *18*, 713–720.
- Rossetti, M., Gregori, S., Hauben, E., Brown, B.D., Sergi, L.S., Naldini, L., and Roncarolo, M.G. (2011). HIV-1-derived lentiviral vectors directly activate plasmacytoid dendritic cells, which in turn induce the maturation of myeloid dendritic cells. *Hum. Gene Ther.* *22*, 177–188.
- Rossi, A., Michelini, Z., Leone, P., Borghi, M., Blasi, M., Bona, R., Spada, M., Grasso, F., Gugliotta, A., Klotman, M.E., et al. (2014). Optimization of mucosal responses after intramuscular immunization with integrase defective lentiviral vector. *PLoS One* *9*, e107377.

- Sakuma, T., Barry, M.A., and Ikeda, Y. (2012). Lentiviral vectors: basic to translational. *Biochem. J.* *443*, 603–618.
- Sato, M., Suemori, H., Hata, N., Asagiri, M., Ogasawara, K., Nakao, K., Nakaya, T., Katsuki, M., Noguchi, S., Tanaka, N., and Taniguchi, T. (2000). Distinct and essential roles of transcription factors IRF-3 and IRF-7 in response to viruses for IFN- α / β gene induction. *Immunity* *13*, 539–548.
- Sauer, J.D., Sotelo-Troha, K., von Moltke, J., Monroe, K.M., Rae, C.S., Brubaker, S.W., Hyodo, M., Hayakawa, Y., Woodward, J.J., Portnoy, D.A., and Vance, R.E. (2011). The N-ethyl-N-nitrosourea-induced Goldenticket mouse mutant reveals an essential function of Sting in the in vivo interferon response to *Listeria monocytogenes* and cyclic dinucleotides. *Infect. Immun.* *79*, 688–694.
- Schlecht, G., Garcia, S., Escriou, N., Freitas, A.A., Leclerc, C., and Dadaglio, G. (2004). Murine plasmacytoid dendritic cells induce effector/memory CD8⁺ T-cell responses in vivo after viral stimulation. *Blood* *104*, 1808–1815.
- Schmidt-Suppran, M., Bloch, W., Courtois, G., Addicks, K., Israël, A., Rajewsky, K., and Pasparakis, M. (2000). NEMO/IKK gamma-deficient mice model incontinentia pigmenti. *Mol. Cell* *5*, 981–992.
- Seth, R.B., Sun, L., Ea, C.K., and Chen, Z.J. (2005). Identification and characterization of MAVS, a mitochondrial antiviral signaling protein that activates NF-kappaB and IRF 3. *Cell* *122*, 669–682.
- Sun, Q., Sun, L., Liu, H.H., Chen, X., Seth, R.B., Forman, J., and Chen, Z.J. (2006). The specific and essential role of MAVS in antiviral innate immune responses. *Immunity* *24*, 633–642.
- Swiecki, M., Gilfillan, S., Vermi, W., Wang, Y., and Colonna, M. (2010). Plasmacytoid dendritic cell ablation impacts early interferon responses and antiviral NK and CD8(+) T cell accrual. *Immunity* *33*, 955–966.
- Takahashi, K. (2001). Development and differentiation of macrophages and related cells: historical review and current concepts. *J. Clin. Exp. Hematop.* *41*, 1–33.
- Thompson, M.R., Kaminski, J.J., Kurt-Jones, E.A., and Fitzgerald, K.A. (2011). Pattern recognition receptors and the innate immune response to viral infection. *Viruses* *3*, 920–940.
- Vargas, J., Jr., Gusella, G.L., Najfeld, V., Klotman, M.E., and Cara, A. (2004). Novel integrase-defective lentiviral episomal vectors for gene transfer. *Hum. Gene Ther.* *15*, 361–372.
- Vigna, E., and Naldini, L. (2000). Lentiviral vectors: excellent tools for experimental gene transfer and promising candidates for gene therapy. *J. Gene Med.* *2*, 308–316.
- Watts, T.H. (2005). TNF/TNFR family members in costimulation of T cell responses. *Annu. Rev. Immunol.* *23*, 23–68.
- Wherry, E.J., and Ahmed, R. (2004). Memory CD8 T-cell differentiation during viral infection. *J. Virol.* *78*, 5535–5545.
- Wherry, E.J., and Kurachi, M. (2015). Molecular and cellular insights into T cell exhaustion. *Nat. Rev. Immunol.* *15*, 486–499.
- Zufferey, R., Dull, T., Mandel, R.J., Bukovsky, A., Quiroz, D., Naldini, L., and Trono, D. (1998). Self-inactivating lentivirus vector for safe and efficient in vivo gene delivery. *J. Virol.* *72*, 9873–9880.

STAR★METHODS

KEY RESOURCES TABLE

REAGENT or RESOURCE	SOURCE	IDENTIFIER
Antibodies		
anti-mouse CD11c/PE-Cy7 (N418)	eBioscience	Cat#25-0114-82; RRID: AB_469590
anti-mouse CD317/APC (eBio927)	eBioscience	Cat#17-3172-82; RRID: AB_10596356
anti-mouse B220/PerCP-Cy5.5 (RA3-6B2)	eBioscience	Cat#45-0452-82; RRID: AB_1107006
anti-mouse CD11b/APC-eF780 (M1/70)	eBioscience	Cat#47-0112-82; RRID: AB_1603193
anti-mouse CD8a/eF450 (53-6.7)	eBioscience	Cat#48-0081-82; RRID: AB_1272198
anti-mouse PDC-TREM/PE (4A6)	BioLegend	Cat#139204; RRID: AB_10613471
anti-mouse ICOS-L/Biotin (HK5.3)	eBioscience	Cat#13-5985-85; RRID: AB_466843
anti-mouse CD69/BV786 (H1.2F3)	BD	Cat#564683; RRID: AB_2738890
anti-mouse CD80/BV650 (16-10A1)	BioLegend	Cat#104731; RRID: AB_11147759
anti-mouse OX40-L/Biotin (RM134L)	eBioscience	Cat#13-5905-85; RRID: AB_466792
anti-mouse H-2K ^b /PE (AF6-88-5)	eBioscience	Cat#12-5958-82; RRID: AB_10598797
anti-mouse CD86/BV650 (GL1)	BioLegend	Cat#105035; RRID: AB_11126147
anti-mouse PDL1/Biotin (M1H5)	eBioscience	Cat#13-5982-85; RRID: AB_466838
anti-mouse I-A ^b /PE (AF6-120.1)	BD	Cat#553552; RRID: AB_394919
anti-mouse CD40/Biotin (3/23)	BD	Cat#553789; RRID: AB_395053
anti-mouse CD54/PE (YN1/1.7.4)	eBioscience	Cat#12-0541-81; RRID: AB_465706
anti-mouse Siglec-H/PE (440c)	eBioscience	Cat#12-0333-82; RRID: AB_10597139
anti-mouse F4/80/Biotin (BM8)	Biolegend	Cat#123105; RRID: AB_893499
streptavidin-BV500	BD	Cat#561419; RRID: AB_10611863
anti-mouse CD3/eF450 (17A2)	eBioscience	Cat#48-0032-82; RRID: AB_1272193
anti-mouse CD19/PE-Cy7 (1D3)	BD	Cat#561739; RRID: AB_10894021
anti-mouse CD27/PE (LG.7F9)	eBioscience	Cat#12-0271-82; RRID: AB_465614
anti-mouse NK1.1/APC (PK-136)	eBioscience	Cat#17-5941-82; RRID: AB_649479
anti-mouse CD3/APC-eF780 (17A2)	eBioscience	Cat#47-0032-82; RRID: AB_1272181
anti-mouse CD4/BUV737 (RM4-5)	BD	Cat#564933; RRID: AB_2732918
anti-mouse CD8a/BUV395 (53-6.7)	BD	Cat#563786; RRID: AB_2732919
anti-mouse CD27/PerCP-eF710 (LG.7F9)	eBioscience	Cat#46-0271-82; RRID: AB_1834447
anti-mouse CD44/APC (IM7)	eBioscience	Cat#17-0441-82; RRID: AB_469390
anti-mouse CD45RA/BV650 (14.8)	BD	Cat#564360; RRID: NA
anti-mouse CD62L/PE-Cy7 (MEL-14)	eBioscience	Cat#25-0621-82; RRID: AB_469633
anti-mouse CCR7/eF450 (4B12)	eBioscience	Cat#48-1971-82; RRID: AB_1944351
anti-mouse PD-1/BV786 (J43)	BD	Cat#744548; RRID: AB_2742319
anti-mouse CD152/PECy7 (UC10-4B9)	Biolegend	Cat#106313; RRID: AB_2564237
anti-mouse CD223/BV650 (C9B7W)	Biolegend	Cat#125227; RRID: AB_2687209
anti-mouse CD366/PerCPCy5.5 (RMT3-23)	Biolegend	Cat#119717; RRID: AB_2571934
anti-mouse CD11c/eF450 (N418)	eBioscience	Cat#48-0114-82; RRID: AB_1548654
anti-mouse B220/PE (RA3-6B2)	Biolegend	Cat#103207; RRID: AB_312992
anti-mouse CD3e/FITC (17A2)	Biolegend	Cat#100203; RRID: AB_312660
anti-mouse CD3/eF660 (17A2)	eBioscience	Cat#50-0032-82; RRID: AB_10598657
anti-mouse CD4/eF450 (GK1.5)	eBioscience	Cat#48-0041-82; RRID: AB_10718983
anti-mouse CD8/PE (53-6.7)	Biolegend	Cat#100707; RRID: AB_312746
H-2K ^b /SIINFEKL-Dextramer/PE	Immudex	Cat#JD2163; RRID: NA

(Continued on next page)

Continued		
REAGENT or RESOURCE	SOURCE	IDENTIFIER
Chemicals, Peptides, and Recombinant Proteins		
synthetic peptide OVA ₂₅₇₋₂₆₄ (SIINFEKL)	NeoMPS	N/A
OVA protein	Calbiochem	N/A
DOTAP Liposomal Transfection Reagent	Roche	Cat#11 202 375 001
<i>in vivo</i> -jetPEI	Polyplus transfection	Cat#201-50G
Diphtheria toxin	Calbiochem	N/A
Critical Commercial Assays		
ProcartaPlex mouse cytokine and chemokine 26Plex immunoassay kit	eBioscience	Cat#EPX260-26088-901
ProcartaPlex Mouse IFN- α and IFN- β 2Plex Assay	eBioscience	Cat#EPX020-22187-901
SV Total RNA Isolation System (modified for DNA preparation)	Promega	N/A
NucleoSpin RNA XS	Machery-Nagel	Cat#740902.50
nCounter Mouse Pan Cancer Immune Profiling Panel	Nanostring technologies	Cat#XT-CSO-MIP1-12
Agilent RNA 6000 Pico Kit	Agilent technologies	Cat#5067-1513
DNeasy Blood & Tissue Kit	QIAGEN	Cat#69504
Experimental Models: Cell Lines		
HeLa cells	ATCC	Cat#CCL-2
B16-F10 cells	Univ. of Massachusetts, Worcester, MA 01655	N/A
B16-OVA cells	Univ. of Massachusetts, Worcester, MA 01655	N/A
Experimental Models: Organisms/Strains		
Mouse: B6.FVB-Tg(Itgax-DTR/GFP)57Lan/J	Jackson Laboratory	Stock No: 004509
Mouse: B6.Cg-Tg(Itgax-cre)1-1Reiz/J	Jackson Laboratory	Stock No: 008068
Mouse: B6;129-Mavstm1Zjc/J	Jackson Laboratory	Stock No: 008634
Mouse: C57BL/6J-Tmem173 < gt > /J	Jackson Laboratory	Stock No: 017537
Mouse: Ikbkgtm1.1Mpa [flox]	Pasteur Institute	Schmidt-Supprian et al., 2000
Mouse: C57BL/6- Tg(CLEC4C-HBEGF)956Cln/J	Jackson Laboratory	Stock No: 014176
Oligonucleotides		
See Table S1 for oligonucleotide information		
Recombinant DNA		
pTY2-CMV-OVA-WPRE	Rossi et al., 2014	N/A
pTY2-CMV-GFP-WPRE	Rossi et al., 2014	N/A
pcHelp/IN-	Rossi et al., 2014	N/A
pHCMV-VSVG	Rossi et al., 2014	N/A
Software and Algorithms		
FlowJo software 9.9.3	Tree Star	N/A
Prism software 6.0	GraphPad	N/A
nSolver Analysis Software 3.0	Nanostring technologies	N/A
Qlucore Omics Explorer 3.0	Qlucore	N/A
R package DESeq2	N/A	Love et al., 2014
Other		
SA Biosciences Data Analysis Web Portal	SABiosciences	http://dataanalysis.sabiosciences.com/pcr/arrayanalysis.php

CONTACT FOR REAGENT AND RESOURCE SHARING

Further information and requests for resources and reagents should be directed to and will be fulfilled by the Lead Contact, Claude Leclerc (claud.leclerc@pasteur.fr).

EXPERIMENTAL MODEL AND SUBJECT DETAILS

In vivo animal studies

Female C57BL/6/J (BL/6) mice were obtained from Charles River. CD11c-Diphtheria Toxin (DT) receptor (DTR) (B6.FVB-Tg(Itgax-DTR/GFP)57Lan/J) (Jung et al., 2002), CD11c-Cre (B6.Cg-Tg(Itgax-cre)1-1Reiz/J) (Caton et al., 2007) transgenic mice, MAVS-deficient (B6;129-Mavstm1Zjc/J) (Sun et al., 2006) and STING-deficient (C57BL/6J-Tmem173 < gt > /J) (Sauer et al., 2011) mice were purchased from The Jackson Laboratory (Bar Harbor, ME). Except MAVS-deficient mice, which were a mix of C57BL/6 and 129/Sv strain, these mice were all on the C57BL/6 background. TLR3- (Alexopoulou et al., 2001), 4- (Hoshino et al., 1999), 7- (Hemmi et al., 2002), 9- (Hemmi et al., 2000), MyD88- (Kawai et al., 1999), IFN receptor 1- (IFNAR) (Müller et al., 1994), IRF3- (Sato et al., 2000), IRF7- (Honda et al., 2005) and IRF3/7-deficient mice, Nemo flox (Ikbkgtm1.1Mpa [flox]) (Schmidt-Suppryan et al., 2000) and BDCA2-DTR (C57BL/6- Tg(CLEC4C-HBEGF)956Cln/J) (Swiecki et al., 2010) transgenic mice were on the C57BL/6 background. All strains were bred in Pasteur Institute facilities under specific and opportunistic pathogen-free conditions (SOPF). All experiments were performed under SPF conditions after acclimation of at least 8 days. Animal studies were approved by the CETEA ethics committee number 89 (Institut Pasteur, Paris, France) and by the French Ministry of Research (MESR 00355.02).

For *in vivo* animal studies, 6 to 12 weeks old female C57BL/6 mice were used as control mice for experiments using deficient mice (MAVS-, STING-, TLR3-, TLR4-, TLR7-, TLR9-, MyD88-, IFNAR-, IRF3-, IRF7- and IRF3/7-deficient mice). These deficient mice were 6 to 12 old weeks, male or female, according to their availability in the animal facilities.

To generate CD11c-DTR → C57BL/6 bone marrow (BM) chimeric mice, 5 weeks old female C57BL/6 mice were irradiated with a single lethal dose of 6 grays, which were then reconstituted with 5×10^6 BM cells from CD11c-DTR mice. BM chimeric mice were kept on antibiotic-supplemented drinking water for 10 days and used 8 weeks after reconstitution. Littermates PBS-treated of the same age and sex were randomly assigned to experimental groups which were DT-treated. The same experimental procedure was used for BDCA2-DTR mice. For the depletion of cDCs or pDCs, CD11c-DTR → C57BL/6 BM chimeric mice or BDCA2- DTR mice, were respectively injected i.p. with 5.2 ng DT (Calbiochem, Merck distributor, Fontenay sous Bois, France) per gramme 1 day before immunization and then every 2 days.

To generate mice with a conditional depletion of the NF-κB pathway in CD11c⁺ cells, CD11c-Cre transgenic mice were first crossed to obtain homozygous transgenic mice and littermate non transgenic mice. Then, these mice were crossed with the Nemo flox mice. At each generation, offspring were genotyped using PCR for CD11c-Cre and for Nemo flox. A first generation of females (F1) was obtained from a Nemo flox⁺ male crossed with homozygous CD11c-Cre transgenic female mice. The F1 females were then crossed with a Nemo flox⁺ male and F2 offspring with flox⁺ and Cre⁺ crossed between them. The offspring obtained from this last crossing (F3; Nemo⁻) were finally used for immunization. Control mice (Nemo⁺) obtained from a male CD11c-Cre littermate crossed with Nemo flox female mice were also immunized.

For tumor challenge, female C57BL/6 mice (6-8 weeks old) purchased from Charles River were kept in pathogen-free condition in the animal facilities at the Istituto Superiore di Sanita (ISS, Rome, Italy) and treated according to European Union guidelines and Italian legislation (Decreto Legislativo 26/2014). All animal studies were authorized by the Italian Ministry of Health and reviewed by the Service for Animal Welfare at ISS (Authorization n. 314/2015-PR of 30/04/2015). All animals were euthanized by CO₂ inhalation using approved chambers, and efforts were made to minimize suffering and discomfort. Twenty-six weeks after immunization with 6×10^6 TUs IDLV-OVA or with IDLV expressing an unrelated antigen, mice were injected subcutaneously with 2×10^5 B16-OVA and the tumor growth was followed. Mice developing tumor larger than 15 mm or showing ulceration were sacrificed.

Cell lines

The cell lines used in this work were HeLa (ATCC, Manassas, VA), B16F10 and B16-OVA cells (obtained from Dr. Louis Sigal, University of Massachusetts, Worcester, MA 01655).

Indeed, to generate positive and negative controls to detect ⁽¹⁾ the presence of the OVA transgene and ⁽²⁾ the integration of the vector, we extracted DNA ⁽¹⁾ from HeLa cells, transduced or not with IDLV-OVA and ⁽²⁾ from B16F10 transduced with integrase-competent LV expressing the ovalbumin (LV-OVA). For that, ⁽¹⁾ 10^5 HeLa adherent cells / well in complete DMEM medium (ATCC) were plated in 6-well plates. The day after, cells were transduced overnight with 1 mL of complete medium containing 1 MOI IDLV-OVA. DNA from HeLa cells transduced with IDLV and non-transduced (ϕ) HeLa cells were extracted on day 3 using the SV Total RNA Isolation System protocol, modified for DNA preparation as previously described (Rossi et al., 2014); ⁽²⁾ 10^5 B16F10 adherent cells in complete DMEM medium were plated in 6-well plates. The day after, cells were transduced overnight with 1 mL of complete medium containing 1 MOI LV-OVA. DNA from the transduced B16F10 cells was extracted at 2 weeks after transduction using the mi-Tissue Genomic DNA Isolation Kit (Metabion International AG, Martinsried, Germany).

For tumor challenge, B16-OVA tumor cells, which are B16 melanoma cells transfected with OVA antigen were kindly provided by L. Rosthein and L. Sigal (University of Massachusetts, Worcester, MA). They were cultured in complete medium supplemented with 2 mg/mL geneticin G418 (Life Technologies) and 60 μg/mL hygromycin B (Roche).

METHOD DETAILS

Reagents

The reagents used for vaccination were the following: the synthetic peptide OVA_{257–264} (SIINFEKL), corresponding to the H-2K^b restricted CTL epitope of ovalbumin (OVA), was purchased from NeoMPS (Strasbourg, France). The OVA protein was obtained from Calbiochem (San Diego, CA). Unmethylated cytosine-guanine class B (CpG-B) motifs (TLR9 ligand-CpG-B 1826 5'-TCC ATG ACG TTC CTG ACG TT-3') were synthesized by Sigma Aldrich (St Quentin Fallavier, France) and DOTAP Liposomal Transfection Reagent was purchased from Roche (Sigma Aldrich distributor, St Quentin Fallavier, France). 5'ppp-dsRNA was purchased from InvivoGen (Toulouse, France) and the *in vivo* nucleic acid delivery *in vivo*-jetPEI was acquired from Polyplus transfection (Illkirch, France).

Lentiviral vector production

Integrase-Deficient Lenviral Vectors (IDLVs) expressing the coding sequence for ovalbumin (see next paragraph) (IDLV-OVA) or GFP (IDLV-GFP) were generated and titered as previously described (Rossi et al., 2014). These doses are expressed as transduction units (TUs) corresponding to the number of functional viral particles in a solution that are capable of transducing a cell and expressing the transgene.

Coding sequence of the OVA protein

ATGgggctccatcggcgcagcaagcatggaatttggttgatgtattcaaggagctcaagtcaccatgccaatgagaacatctct actgcccattgccatcatgtcagctct agccatggtataccctgggtgcaaaagacagcaccaggacacagataaataaggtgttcgct ttgataaactccaggattcggagacagtattgaagctcagtggtgacacatctg taaacgttcactctcacttagagacatcctcaaccaa atcaccaaaccaaatgatgtttattcgttcagccttgccagtagactttatgtgaagagagataccaatcctgcccaga atacttgcagtg tggaaggaactgtatagaggagcctggaacatcaactttcaaacagctgcagatcaagccagagagctcatcaattcctgggtag aaagtcagacaaa tggattatcagaatgtccttcagccaagctcctggattctcaaacctgcaatggttctggttaatgccattgtctc aaaggactgtgggagaaacatttaaggatgaagacaca caagcaatgccttcagagtgactgagcaagaagcaaacctgtgcagatgatgtaccagattggtttattagagtggcacaatggcttctgagaaaaatgaagatcctggagctt ccatttgccagtgggacaatgag catgttggtgctgtgctgatgaagctcaggccttgagcagcttgagagtataatcaacttgaaaaactgactgaatggaccagttcta atg ttatggaagagaggaagatcaaagtgtactacctcgcataagatggaggaaaaatacaacctcacatctgtcttaattggctatgg gcattactgacgtgtttagctctcagccaa tctgtctggcatctcctcagcagagagcctgaagatatctcaagctgtccatgcagcacat gcagaaatcaatgaagcaggcagagaggtgtagggtcagcagaggtggag tggatgctgaagcgtctctgaagaatttagggc tgaccatcattcctctctgtatcaagcacatgcacaaccaacgccttctctctttggcagatgtgttcccctctagatgcat gctcag cggccgcagtgatggtgatctgcagaattcggcttggataatcaacctctggattacaaaatttgtaagatTGA

Flow cytometry analysis

Spleen cells were washed, incubated with a Fc block, and stained with various mAbs. Cells were then washed and acquired using an LSR Fortessa cytometer (BD Biosciences, Rungis, France) and analyzed with FlowJo Software (Tree Star, Ashland, OR).

For all flow cytometry analysis, fluorochrome-labeled Abs against murine cell surface Ags were from BD Biosciences (Le Pont de Claix, France), BioLegend (Ozyme distributor, Saint Quentin en Yvelines, France) and eBioscience (ThermoFisher Scientific, France). The Fc block is a mAb against mouse FcR produced by BioXCell (West Lebanon, NH).

To characterize DC subsets, the following mix of antibodies were used: one pre-mix with anti-CD11c/PE-Cy7 (N418), anti-CD317/APC (eBio927), anti-B220/PerCP-Cy5.5 (RA3-6B2), anti-CD11b/APC-eF780 (M1/70) and anti-CD8a/eF450 (53-6.7) mAbs as well as mix1 composed of anti-PDC-TREM/PE (4A6), anti-ICOS-L/Biotin (HK5.3) followed by an additional incubation with streptavidin-BV500 and anti-CD69/BV786 (H1.2F3); mix2 composed of anti-CD80/BV650 (16-10A1), anti-OX40-L/Biotin (RM134L) followed by an additional incubation with streptavidin-BV500 and anti-H-2Kb/PE (AF6-88-5); mix3 composed of anti-CD86/BV650 (GL1), anti-PDL1/Biotin (M1H5) followed by an additional incubation with streptavidin-BV500 and anti-I-Ab/PE (AF6-120.1) and mix4 composed of anti-CD40/Biotin (3/23), streptavidin-BV500 and anti-CD54/PE (YN1/1.7.4).

To control DC depletion, spleen cells were stained with a first mix for macrophages and DC: anti-CD8a/eF450, anti-CD317/APC, anti-CD11c/PE-Cy7, anti-B220/PerCP-eF710, anti-Siglec-H/PE (440c), anti-CD11b/APC-eF780 and anti-F4/80/Biotin (BM8) mAbs followed by an additional incubation with streptavidin-BV500 and a second mix for NK cells: anti-CD3/eF450 (145-2C1), anti-CD19/PE-Cy7 (1D3), anti-CD27/PE (LG.7F9), anti-NK1.1/APC (PK-136) and anti-CD11b/APC-eF780.

To characterize the OVA-specific CD8⁺ T cell phenotype, spleens were removed seven days and one month after immunization. 3x10⁶ cells were washed, incubated for 10 min at RT with 10 μL of H-2K^b/SIINFEKL-Dextramer (Immunex, Copenhagen, Denmark) followed by an additional incubation of 20 min at 4°C with Fc block, anti-CD3/APC-eF780 (17A2), anti-CD4/BUV737 (RM4-5), anti-CD8a/BUV395 (53-6.7), anti-CD27/PerCP-eF710 (LG.7F9), anti-CD44/APC (IM7), anti-CD45RA/BV650 (14.8), anti-CD62L/PE-Cy7 (MEL-14) and anti-CCR7/eF450 (4B12) mAbs (Figure 1G) or anti-CD3/FITC (17A2), anti-CD4/eF450 (GK1.5), anti-CD8a/PE (53-6.7), anti-PD-1/BV786 (J43), anti-CD152/PE-Cy7 (UC10-4B9), anti-CD223/BV650 (C9B7W) and anti-CD336/PerCP-Cy5.5 (RMT3-23) mAbs (Figure S2C). Cells were then washed, filtered and acquired using an LSR Fortessa cytometer and analyzed with FlowJo Software.

Analysis of cytokine and chemokine production

Cytokine and chemokine concentration in the mouse sera was assessed with Luminex MagPIX technology using the ProcartaPlex mouse cytokine and chemokine 26Plex immunoassay kit from eBioscience (eBioscience, Paris, France). IFN-α and IFN-β concentrations were determined using the ProcartaPlex Mouse IFN-α and IFN-β 2Plex Assay from eBioscience.

In vivo killing assay

Mice were injected i.v. with PBS, 10^6 TUs IDLV-OVA, 100 μ g OVA with 25 μ g 5'ppp-dsRNA and 4 μ L *in vivo*-jetPEI, or 100 μ g OVA with 30 μ g CpG-B 1826 plus 60 μ g DOTAP. The percentage of specific lysis was assessed by an *in vivo* killing assay as previously described (Hervas-Stubbs et al., 2007). Naive syngeneic splenocytes were pulsed with the OVA_{257–264} peptide (1 ng/ml) and labeled with a high concentration (2.5 μ M) of CFSE (Molecular Probes, Fisher Scientific distributor, Illkirch, France). The non-pulsed control population was labeled with a low concentration (0.25 μ M) of CFSE. CFSE^{high}- and CFSE^{low}-labeled cells were mixed in a 1:1 ratio and injected i.v. into the mice 6 days after the immunization. The number of CFSE-positive cells remaining in the spleen after 19 hours was determined by flow cytometry, and the percentage of specific lysis was calculated as follows: % specific lysis = $100 - [100 \times (\%CFSE^{high} \text{ immunized mice} / \%CFSE^{low} \text{ immunized mice}) / (\%CFSE^{high} \text{ naive mouse} / \%CFSE^{low} \text{ naive mouse})]$.

IFN- γ ELISPOT assay

Mice were injected i.v. with PBS, 10^6 TUs IDLV-OVA, 100 μ g OVA with 25 μ g 5'ppp-dsRNA and 4 μ L *in vivo*-jetPEI, or 100 μ g OVA with 30 μ g CpG-B 1826 plus 60 μ g DOTAP. The frequency of OVA_{257–264}-specific IFN- γ -producing cells was determined by an enzyme-linked immunospot (ELISPOT) assay, as previously described (Schlecht et al., 2004). Ninety-six-well Multiscreen-HA sterile plates (Millipore, Molsheim, France) were coated with purified anti-IFN- γ mAbs (Murine IFN- γ ELISpot Pair from Diaclone). Plates were washed and blocked with complete culture medium for 2 hours before adding the cells. Various numbers of splenocytes from immunized and control mice were then added (2 to 4 $\times 10^5$ per well) in the presence or absence of 10 μ g/mL of OVA_{257–264} peptide. The cells were cultured O/N at 37°C. They were then washed and the biotinylated mAbs were added (Murine IFN- γ ELISpot Pair from Diaclone) in a solution of PBS 1% BSA. One hour and half later, the plates were washed and streptavidin-alkaline phosphatase (AKP) was added to the wells in a solution of PBS 1% BSA. One hour later, the plates were washed and BCIP/NBT (5-bromo-4-chloro-3-indolyl phosphate/nitro blue tetrazolium substrate; Sigma-Aldrich, 100 μ L) was added to each well. Ten minutes later, the revelation was stopped with water. The spots were counted using the automated Bioreader-3000 pro counter (Bioreader, Karben, Germany). For each mouse, the number of peptide-specific IFN- γ -producing cells was determined by calculating the difference between the number of spots generated in the absence and in the presence of the OVA_{257–264} peptide. Results are expressed as spot-forming cells (SFCs) per number of splenocytes in the wells.

PCR arrays

CD11c⁺CD3e⁺B220⁺CD317⁻ splenic cells from immunized mice were first magnetically sorted with anti-CD11c-Beads (Miltenyi Biotec, Paris, France) and then by FACS ARIA after labeling with anti-CD11c/eF450 (N418), anti-B220/PE (RA3-6B2), anti-CD317/APC (eBio927) and anti-CD3e/FITC (17A2) antibodies. The purity was always > 96.3% of live cells. RNA from purified CD11c⁺ cells was extracted from cell lysates with the RNeasy Plus microkit (QIAGEN, Courtaboeuf, France). cDNA was generated using a RT2 First Strand Kit and quantified using the RT2 Profiler Mouse antiviral responses and NF- κ B signaling pathway PCR arrays (SABiosciences, QIAGEN, Courtaboeuf, France), according to the manufacturer's instructions. The results were analyzed using the SA Biosciences Data Analysis Web Portal (<http://dataanalysis.sabiosciences.com/pcr/arrayanalysis.php>) and expressed as fold regulation compared to PBS-treated mice.

Genotyping of mice with NEMO-deficient CD11c⁺ cells

To generate mice with a conditional depletion of the NF- κ B pathway in CD11c⁺ cells, offspring were genotyped using PCR for CD11c-Cre and for Nemo flox at each generation.

DNA was extracted from biopsies of the offspring obtained after crossing CD11c-Cre mice with Nemo flox mice using the DNeasy Blood & Tissue Kit (QIAGEN, Courtaboeuf, France).

Samples were included in PCR analysis to detect the presence of:

- CD11c-Cre using a primer pair spanning the transgene (oIMR7841: 5'-ACT TGG CAG CTG TCT CCA AG-3'; oIMR7842: 5'-GCG AAC ATC TTC AGG TTC TG-3') and an internal positive control (oIMR8744: 5'-CAA ATG TTG CTT GTC TGG TG-3'; oIMR8745: 5'-GTC AGT CGA GTG CAC AGT TT-3'). Reactions were performed with 2 μ L of genomic DNA in a 10 μ L total volume containing 1x reaction buffer (Invitrogen, Fisher Scientific distributor, Illkirch, France), 2 mM MgCl₂ (Invitrogen), 0.2 mM of each dNTP (Roche, Sigma Aldrich distributor, St Quentin Fallavier, France), 1 μ M each of the forward and reverse transgene primers, 0.5 μ M each of the forward and reverse internal positive control primers and 1 unit of Platinum Taq polymerase (Invitrogen). The PCR conditions were as follows: 1 cycle of 3 min at 94°C, followed by 35 cycles of 30 s at 94°C, 1 min at 64°C, 1 min at 72°C with a final extension step of 2 min at 72°C in a CFX96 BioRad Thermocycler. PCR products were analyzed by gel electrophoresis on 2% agarose gels stained with ethidium bromide. The resulting PCR product sizes were 313 bp for the transgene and 200 bp for the internal positive control.
- Flox using the following primers (Nemo 209: 5'-CGT GGA CCT GCT AAA TTG TCT-3'; Nemo 210: 5'-ATC ACC TCT GCA AAT CAC CAG-3'; Nemo 211: 5'-ATG TGC CCA AGA ACC ATC CAG-3'), and reactions were performed with 2 μ L of genomic DNA in a 10 μ L total volume containing 1x reaction buffer (Invitrogen, Fisher Scientific distributor, Illkirch, France), 2 mM MgCl₂ (Invitrogen), 0.2 mM of each dNTP (Roche, Sigma Aldrich distributor, St Quentin Fallavier, France), 0.2 μ M each of the primers and 1 unit of Platinum Taq polymerase (Invitrogen). PCR conditions were: 1 cycle of 2 min at 94°C, followed by 30 cycles of 30 s

at 94°C, 30 s at 60°C, 30 s at 72°C with a final extension step of 5 min at 72°C in a CFX96 BioRad Thermocycler. PCR products were analyzed by gel electrophoresis on ethidium bromide 2% agarose gel. PCR product sizes were 301 bp for the WT and 446 bp for the flox and 644 bp for the KO.

As the PCR for CD11c-Cre does not distinguish hemizygous from homozygous transgenic animals, a quantitative PCR was performed using primer pairs spanning the transgene (oIMR1084: 5'-GCG GTC TGG CAG TAA AAA CTA TC-3'; oIMR1085: 5'-GTG AAA CAG CAT TGC TGT CAC TT-3'), an internal positive control (oIMR1544: 5'-CAC GTG GGC TCC AGC ATT-3'; oIMR3580: 5'-TCA CCA GTC ATT TCT GCC TTT G -3') and internal control and transgenic probes (TmoIMR0105: 5'-Cy5-CCA ATG GTC GGG CAC TGC TCA A-BHQ2-3'; 13593: 5'-6-FAM-AAA CAT GCT TCA TCG TCG GTC CGG- BHQ1-3'). Reactions were performed with 20 ng of genomic DNA in a 20 μ L total volume containing 1x iTaq (BioRad, Marnes-la-Coquette, France), 0.22 μ M each of the forward and reverse transgene primers, 1.1 μ M of the forward internal positive control primer, 0.44 μ M of the reverse internal positive control primer and 0.16 μ M each of the probes. The PCR conditions were: 1 cycle of 3 min at 95°C, followed by 40 cycles of 10 s at 95°C and 1 min at 60°C in a CFX96 BioRad Thermocycler. The transgene genotype was determined by comparing Δ Ct values of each sample.

Transcriptomic analysis

C57BL/6 mice were injected i.v. with PBS, 10^6 TU IDLV-OVA or OVA plus CpG. Seven days later, CD8⁺ T cells and CD8⁺ dextramer⁺ T cells from the spleens of immunized mice were first magnetically sorted using CD8a⁺ T Cell Isolation Kit, mouse (Miltenyi Biotec, Paris, France) and then by FACS ARIA after labeling with anti-CD3/eF660 (17A2), anti-CD4/eF450 (GK1.5), anti-CD8/PE (53-6.7) and H-2K^b/SIINFEKL-Dextramer. The purity of CD8⁺ T cells and CD8⁺ dextramer⁺ T cells was always > 99.7% and > 95.1% of live cells, respectively.

C57BL/6 mice were injected i.v. with PBS, $5 \cdot 10^6$ TU IDLV-OVA or OVA plus CpG. Eighteen hours later, CD11c^{high} B220⁻ splenic cells were first magnetically sorted with Pan Dendritic Cell Isolation Kit from Miltenyi Biotec following manufacturer's instruction and then by FACS ARIA after labeling with anti-CD11c/PE-Cy7 (N418) and anti-B220/PerCP-Cy5.5 (RA3-6B2) fluorescent antibodies. The purity was always > 95.3% of live cells.

RNA was extracted from cell lysates (30 000 to 250 000 cells) of vaccinated mice with the NucleoSpin RNA XS (Machery-Nagel, Hoerd, France), and the expression of genes involved in the immune response was assessed using Nanostring technologies with the nCounter Mouse Pan Cancer Immune Profiling Panel, according to the manufacturer's instructions. RNA quality was evaluated using Agilent RNA 6000 Pico Kit (Agilent technologies, Courtaboeuf, France) according to the manufacturer's instructions, and all samples with RIN values less than 7 were excluded.

For the analysis of genes expressed by OVA-specific CD8⁺ T cells, the results were analyzed using nSolver Analysis Software 3.0 and QluCore Omics Explorer 3.0. Normalized data were exported from nSolver Analysis Software 3.0 after a negative control subtraction, positive control normalization and CodeSet content normalization using 5/20 housekeeping genes (*Eif2b4*, *Nubp1*, *Sap130*, *Sdha* and *Sf3a3*). Differentially expressed genes were analyzed using QluCore Omics Explorer 3.0, filtered by a Multi Group Comparison with a q value = 0.05 and using a t- test comparison.

For the analysis of genes expressed by cDCs, normalization on endogenous genes and analysis (Figure S8) was performed using R package DESeq2 (Love et al., 2014). Default settings of the DESeq2 package were used for the analysis of differentially expressed genes (Wald test followed by Benjamini Hochberg's adjustment, selection of genes with adjusted p value < 0.05). The visualization of specific genes (Figure S9) was performed from normalized data exported from nSolver Analysis Software 3.0 after a negative control subtraction, positive control normalization and CodeSet content normalization using 8/20 housekeeping genes having at least an average count above 100 (*Polr2a*, *Hprt*, *Gusb*, *Eef1g*, *Tubb5*, *Oaz1*, *Ppia* and *Rpl19*).

OVA transgene and vector integration analysis

In order to evaluate the presence of the OVA transgene and the integration of the vector, DNA was extracted using the SV Total RNA Isolation System protocol modified for DNA preparation as described previously (Rossi et al., 2014). In brief, 2 important changes in the protocol allow the separate isolation of DNA and RNA, which are the vortexing of the sample during the lysis steps, and the addition of ethanol in two separate steps. When genomic DNA isolation is desired, two vortexing steps facilitate the liberation of genomic DNA from the cell debris so that it can be precipitated by the addition of ethanol. The addition of ethanol in two steps allows for the isolation of DNA after the first ethanol addition, while RNA passes through the SV column. The addition of ethanol to the flowthrough allows the isolation of RNA on a second SV System membrane (Otto et al., 1998).

All samples supported the amplification of the mouse glyceraldehyde 3-phosphate dehydrogenase gene (G3PDH using primer pair GlymoFor: 5'-TGA AGG TCG GTG TGA ACG GAT TTG GC-3'; GlymoRev: 5'-CAT GTA GGC CAT GAG GTC CAC CAC-3'). Reactions were performed on 100 ng of genomic DNA in a 25 μ L total volume containing 1x reaction buffer (Invitrogen, Fisher Scientific distributor, Illkirch, France), 2 mM MgCl₂ (Invitrogen), 0.2 mM of each dNTP (Roche, Sigma Aldrich distributor, St Quentin Fallavier, France), 0.1 μ M each of the forward and reverse primers and 1 unit of Platinum Taq polymerase (Invitrogen). The PCR conditions were: 1 cycle of 5 min at 95°C, followed by 35 cycles of 30 s at 95°C, 30 s at 60°C, and 30 s at 72°C with a final extension step of 10 min at 72°C in a CFX96 BioRad Thermocycler. Then, all samples were included in subsequent PCR analysis.

The detection of the presence of the OVA transgene was performed as follow. In the first step of amplification, a primer pair spanning the OVA sequence (OVAnewF1: 5'-TTC AGC CAA GCT CCG TGG ATT C-3'; OVAnewR1: 5'-TCA GGC AAC AGC ACC AAC ATG

C-3') was used, and reactions were performed on 200 ng of genomic DNA in a 50 μ L total volume containing 1x reaction buffer (Invitrogen), 2 mM MgCl₂ (Invitrogen), 0.4 mM of each dNTP (Roche), 0.4 μ M each of the forward and reverse primers and 1 unit of Platinum Taq polymerase (Invitrogen). The PCR conditions were as follows: 1 cycle of 5 min at 94°C, followed by 35 cycles of 30 s at 94°C, 30 s at 60°C, 30 s at 72°C with a final extension step of 10 min at 72°C in a CFX96 BioRad Thermocycler. After the first amplification, a nested PCR was performed on 5 μ L of the first PCR product in a 50 μ L final volume using the two internal primers in the OVA sequence described above (OVAnewF1/OVAnewR1).

The integrated vector sequence was evaluated using a modified B2-PCR assay (Negri et al., 2007). In the first step of amplification, one primer pair based on the murine B2 family of short interspersed elements (B2AS: 5'-ATA TGT AAG TAC ACT GTA GC-3') was used with one primer in the central polypurine tract sequence of the vector (cPPT: 5'-TCA GTA CAA ATG GCA GTA TTC ATC C-3'). Reactions were performed on 500 ng of genomic DNA in a total volume of 50 μ L containing 1x reaction buffer (Invitrogen), 2 mM MgCl₂ (Invitrogen), 0.4 mM of each dNTP (Roche), 0.4 μ M each of the forward and reverse primers and 1 unit of Platinum Taq polymerase (Invitrogen). The PCR conditions were as follows: 1 cycle of 1 min at 94°C, followed by 35 cycles of 30 s at 94°C, 30 s at 55°C, 15 min at 68°C, with a final extension step of 10 min at 72°C in a CFX96 BioRad Thermocycler. After the first amplification, a nested PCR was performed on 5 μ L of the first PCR product in a 50 μ L final volume using the two internal primers in the OVA sequence described above (OVAnewF1/OVAnewR1).

All the above PCR products were analyzed by gel electrophoresis on ethidium bromide 1% agarose gel. Sizes of PCR products were 983 bp for the GlymoFor/GlymoRev primer pair and 259 bp for the OVAnewF1/OVAnewR1 primer pair.

QUANTIFICATION AND STATISTICAL ANALYSIS

All data were statistically analyzed by an unpaired two-tailed t test using Prism software (GraphPad). ns, $p > 0.05$; * $p < 0.05$, ** $p < 0.01$, *** $p < 0.001$, **** $p < 0.0001$. The results represent the means \pm SEM of cumulative data for a given number of mice per group and experiments. These information can be found in the figure legends.